Landscape#scale plant water content and carbon flux behavior following moisture pulses: from dryland to mesic environments

Water Resources Research

Key Points:

- Ecosystem carbon fluxes and plant water content are sensitive to individual summer soil moisture pulses across dry to humid US biomes
- Ecosystem carbon uptake and plant water content increase following moisture pulses more frequently in drier biomes
- Unlike mesic vegetation, dryland vegetation responses vary depending on pulse magnitudes and antecedent moisture conditions

Supporting Information:

- Supporting Information S1

Correspondence to:
A. F. Feldman,
afeld24@mit.edu

Landscape-Scale Plant Water Content and Carbon Flux Behavior Following Moisture Pulses: From Dryland to Mesic Environments

Andrew F. Feldman[1] , **Apisada Chulakadabba[2]** , **Daniel J. Short Gianotti[1]** , **and Dara Entekhabi[1]**

[1]Department of Civil and Environmental Engineering, Massachusetts Institute of Technology, Cambridge, MA, USA
[2]John A. Paulson School of Engineering and Applied Sciences, Harvard University, Cambridge, MA, USA

Abstract Rain pulses followed by interstorm drying periods are the fundamental units of water input into ecosystems on subweekly time scales. It is essential to understand landscape-scale vegetation responses on these unit time scales as they may describe sensitivity of landscape water, carbon, and energy cycles to shifts in rainfall intensity and frequency, even if the average seasonal precipitation remains unchanged. Because pulse investigations are primarily carried out in drylands, little is known about the characteristics and extent of ecosystem plant pulse responses across the broader range of climates and biomes. Using satellite-based plant water content (from vegetation optical depth) and plant carbon uptake observations from eddy covariance towers across the continental United States climate gradient (dry to humid), we characterize large-scale plant carbon and water uptake responses to rain pulses during spring and summer months. We find that while all ecosystems in the study region show discernable plant water content and carbon flux responses to rain pulses, drier ecosystems exhibit more frequent and longer duration responses. Unlike mesic environments, drylands show significantly different responses under varying antecedent soil moisture and pulse magnitude conditions; the largest water and carbon uptakes follow large pulses on initially wet soils. We detect soil moisture thresholds primarily in drylands, which can partly explain dryland vegetation's different responses under dry and wet conditions. We conclude that vegetation responds to individual pulses of water availability across all climates and therefore a range of ecosystems are sensitive to rainfall distributions beyond simple seasonal precipitation totals.

1. Introduction

Rain pulses provide major inputs of plant available soil water to ecosystems on subweekly scales (Yang et al., 2008). A soil moisture drydown period follows these pulses where soil water is lost through transpiration, soil evaporation, and drainage. After accounting for seasonal modes of water input (i.e., snowmelt), these fundamental pulse time units can additively scale up to describe the annual water cycle at a location (Eagleson, 1978). Given that vegetation exerts a strong control on the global water, carbon, and energy cycles (Jasechko et al., 2013), it is essential to understand terrestrial biosphere behavior on this time scale to, for example, address how rainfall regimes and their changes impact these cycles (Knapp et al., 2002). However, seasonal and annual-scale environmental controls on plant productivity have received more attention (Nemani et al., 2003). We therefore have inadequate knowledge of general plant pulse dynamics and their influence on seasonal and annual vegetation behavior across biomes.

Primarily, only dryland ecosystems have been evaluated in the context of pulsed water inputs (Collins et al., 2014; Schwinning et al., 2004). Dryland vegetation has been hypothesized to be driven by infrequent, unpredictable rain pulses under a pulse-reserve paradigm (Noy-Meir, 1973). This paradigm states that, after rainfall, plants upregulate (increasing sensitivity to external stimuli) with growth and carbohydrate storage, followed by depletion of reserves (Reynolds et al., 2004). Continental-scale evidence exists for this paradigm (Feldman et al., 2018). While field studies have not directly assessed such growth and storage mechanisms (Collins et al., 2014), they have instead evaluated leaf gas exchange and plant hydraulic (i.e., via predawn water potential) responses to rain pulses (Huxman, Snyder, et al., 2004; Sala & Lauenroth, 1982; Williams et al., 2009). Overall, these studies generally agree that small rain events induce ecosystem respiration efflux responses (e.g., the "Birch" effect, Jarvis et al., 2007) and larger rain events additionally result in great-

er water uptake, transpiration, and primary production responses (Chen et al., 2009; Q. Guo et al., 2016; Schwinning et al., 2004; Tang et al., 2018; Xu et al., 2004). Some studies note that antecedent soil moisture conditions explain differences in response magnitude and duration (J. S. Guo and Ogle, 2019; Potts et al., 2006; Tang et al., 2018). However, there have been few efforts to reconcile whole-plant pulse responses beyond individual sites (Ogle & Reynolds, 2004; Reynolds et al., 2004). As such, calls to scale leaf to ecosystem plant pulse behavior and evaluate pulse behavior beyond drylands (i.e., woody vegetation in mesic regions) remain relatively unaddressed (Weltzin & Tissue, 2003; Weltzin et al., 2003).

Scaling up plant behavior beyond drylands is becoming possible with recent satellite missions and streamlined field tower networks. Since the 1980s, remote sensing missions have allowed large-scale characterization of landscape-scale (km scales) vegetation behavior. However, cloud cover sensitivity of widely used optical and thermal satellite-based sensors hinders vegetation sampling periods of less than a week. Therefore, understanding daily landscape-scale plant behavior, especially in the context of pulses, has been limited. Microwave remote sensing missions, insensitive to cloud cover, overcome these limitations with 1–3-day simultaneous retrievals of surface soil and plant water content (Entekhabi et al., 2010; Kerr et al., 2010; Smith et al., 2019). While at a low spatial resolution (~30 km), these observations provide an opportunity to assess subweekly landscape-scale plant pulse-response dynamics. These data sets show promise in evaluating the 1–3 days evolution of vegetation behavior as a recent study found that plant water content increases following soil moisture pulses, signifying plant water uptake (Feldman et al., 2018). Furthermore, with the streamlining and greater availability of eddy covariance towers, multiyear records of hourly ecosystem-scale (100-m scales) carbon flux measurements are also available across many land cover types (Pastorello, 2020). These measurements also have been used to reveal much about carbon pulse dynamics primarily in drylands (Huxman, Cable, et al., 2004; Kurc & Small, 2007; Potts et al., 2006; Roby et al., 2020). Therefore, these plant water content and carbon flux measurements show promise in providing complementary information to assess plant pulse behavior across climates and biomes, without process-model assumptions.

Here, using satellite plant water content and tower-based carbon flux measurements in the continental United States, we aimed to address two questions: (I) what are the plant water content and carbon flux responses to individual rain pulses across climate gradients (dry to humid)? (II) How sensitive is the plant water content and carbon flux behavior to pulse characteristics, specifically antecedent moisture and pulse magnitude? We evaluated the subweekly responses following individual rain pulses using these spatially integrated vegetation observations. The common expectation is that dryland plants show subweekly water uptake and carbon assimilation responses to rain pulses, due to reliance on near-surface soil moisture (Reynolds et al., 2004). Mesic environment vegetation may instead rely more on seasonal rootzone moisture variations with greater sensitivity to temperature and incoming radiation (Madani et al., 2017; Nemani et al., 2003). Our analysis was conducted during the continental US spring and summer when plants are generally phenologically active with less prevalent low temperature limitations (Kurc & Small, 2007; Loik, 2007; Pockman & Small, 2010; Potts et al., 2006).

2. Methodology

2.1. Data Sets

Within our study domain of the continental United States, we used all available FLUXNET eddy covariance tower (Tier 1) measurements of net ecosystem exchange and surface soil moisture (0–5 cm depth) (Pastorello, 2020). Net ecosystem exchange was converted to net ecosystem production (NEP) where positive NEP represents land surface carbon uptake. We also used the partitioned gross primary production (GPP) and ecosystem respiration (R_e) products from FLUXNET to assess the role of R_e (references in Table 1). Daily NEP values are reported here as averaged daytime measurements between 10 a.m. and 4 p.m. Soil moisture values were averaged over the full day. Sites that are without NEP and soil moisture measurements and those that are irrigated, disturbed by fire, or in wetlands were not included. In total, 36 sites were used in our analysis (Table 1).

Within the same domain, we also used Soil Moisture Active Passive (SMAP) satellite-observed surface soil moisture (~5 cm) and vegetation optical depth (VOD) from April 2015 to March 2019 posted on a 9-km grid (Entekhabi et al., 2010; Konings et al., 2016). The SMAP satellite makes observations near 6 a.m. local time, reflecting predawn soil and plant water content conditions. Details of the satellite parameter

Table 1
FLUXNET Eddy Covariance Towers (Tier 1 Data Only) Organized in Order of Increasing Mean Annual Rainfall

Site name	Start year	End year	Latitude	Longitude	Land cover	MAP (mm/ year)	Pulses identified (April–September)	Reference
US-Sta	2005	2009	41.4	−106.8	OSH	308*	8	Reed et al. (2018)
US-Whs	2007	2014	31.74	−110.05	OSH	320	50	Scott et al. (2015)
US-SRC	2008	2014	31.91	−110.84	MF	330	42	Cavanaugh et al. (2011)
US-Cop	2001	2007	38.09	−109.39	GRA	352*	16	Bowling (2007)
US-SRM	2004	2014	31.82	−110.87	WSA	380	61	Scott et al. (2015)
US-Lin	2009	2010	36.36	−119.84	CRO	387*	19	Fares et al. (2012)
US-Wkg	2004	2014	31.74	−109.94	GRA	407	64	Scott et al. (2015)
US-SRG	2008	2014	31.79	−110.83	GRA	420	34	Scott et al. (2015)
US-Tw2	2012	2013	38.1	−121.64	CRO	421	1	Knox et al. (2015)
US-Tw3	2013	2014	38.12	−121.65	CRO	421	2	Oikawa et al. (2017)
US-Me6	2010	2014	44.32	−121.61	ENF	494	1	Ruehr et al. (2012)
US-Me2	2002	2014	44.45	−121.56	ENF	523	27	Law et al. (2004)
US-Ton	2001	2014	38.43	−120.97	WSA	559	34	Baldocchi et al. (2004)
US-Var	2000	2014	38.41	−120.95	GRA	559	24	Baldocchi et al. (2004)
US-Me5	2002	2014	44.44	−121.57	ENF	591	2	Law et al. (2004)
US-Me1	2004	2005	44.58	−121.5	ENF	705	2	Law et al. (2004)
US-Me3	2002	2014	44.32	−121.61	ENF	719	6	Vickers et al. (2009)
US-Ne3	2001	2013	41.18	−96.44	CRO	784	44	Richardson et al. (2006)
US-WCr	1999	2014	45.81	−90.08	DBF	787	105	Cook et al. (2004)
US-NR1	1998	2014	40.03	−105.55	ENF	800	50	Burns et al. (2015)
US-UMB	2000	2014	45.56	−84.71	DBF	803	123	Gough et al. (2013)
US-UMd	2007	2014	45.56	−84.7	DBF	803	70	Gough et al. (2013)
US-LWW	1997	1998	34.96	−97.98	GRA	805	18	Meyers (2001)
US-Pfa	1995	2014	45.95	−90.27	MF	823	68	Davis et al. (2003)
US-Syv	2001	2014	46.24	−89.35	MF	826	38	Desai et al. (2005)
US-ARM	2003	2012	36.61	−97.49	CRO	843	74	Raz-Yaseef et al. (2015)
US-Oho	2004	2013	41.55	−83.84	DBF	849	23	Chu et al. (2016)
US-AR1	2009	2012	36.43	−99.42	GRA	900	16	Billesbach et al. (2012a)
US-AR2	2009	2012	36.64	−99.6	GRA	900	10	Billesbach et al. (2012b)
US-ARc	2005	2006	35.55	−98.04	GRA	900	14	Billesbach et al. (2012b)
US-MMS	1999	2014	39.32	−86.41	DBF	1,032	159	Roman et al. (2015)
US-Me4	2002	2014	44.5	−121.62	ENF	1,039	1	Law et al. (2004)
US-GLE	2004	2014	41.37	−106.24	ENF	1,200	34	Frank et al. (2014)
US-Blo	1997	2007	38.9	−120.63	ENF	1,226	19	Goldstein et al. (2000)
US-KS2	2003	2006	28.61	−80.67	CSH	1,294	37	Li et al. (1999)
US-Goo	2002	2006	34.25	−89.87	GRA	1,426*	25	Hollinger et al. (2010)

Irrigated, wetland, or disturbed sites are not included. Land cover type abbreviations: GRA, grassland; CRO, cropland; ENF, evergreen needleleaf forest; DBF, deciduous broadleaf forest; MF, mixed forest; CSH, closed shrubland; OSH, open shrubland; WSA, woody savanna. *MAP from GPM precipitation product was used due to missing value. Note that 10 cm soil moisture was used at the US-Cop site as 5 cm soil moisture was unavailable. Locations are shown in Figure S1.

retrieval technique (called the multitemporal dual channel algorithm) and uncertainty can be found in Konings et al. (2016) and Feldman et al. (2018). SMAP satellite soil moisture closely resembles in situ soil moisture dynamics at core validation sites primarily across the study domain (Chan et al., 2016; Feldman

et al., 2018). While robustly estimated, the VOD product has yet to undergo thorough ground validation (Konings et al., 2016). VOD represents a unitless measure of attenuation of microwave emission through a canopy and has been found to be linearly proportional to plant water content (Jackson & Schmugge, 1991; Momen et al., 2017). Direct and equivalent field measurements of integrated plant water content are not available. However, the time-averaged VOD correlates strongly with vegetation density and height (Brandt et al., 2018). Furthermore, VOD temporal dynamics compare to predawn water potential (leaf, xylem, etc.), an independent satellite VOD product, and are complementary to leaf area index (Feldman et al., 2018; Momen et al., 2017; Tian et al., 2018; Zhang et al., 2019). For the primary analysis, we evaluated satellite-based VOD and tower-based estimates of NEP between April 1st and September 30th in available years, representing Northern Hemisphere spring and summer seasons.

We computed mean annual precipitation (MAP) from the satellite Global Precipitation Measurement (GPM) IMERG product (Huffman, 2015) to assess satellite-based vegetation behavior across the dry to humid climate gradient in the United States. Similarly, FLUXNET precipitation was also used to quantify MAP corresponding to flux tower vegetation data across this climate gradient. For four FLUXNET sites that do not have a ground-based MAP estimate available (see Table 1), we used the MAP estimate from GPM IMERG over the SMAP time period. Since MAP was primarily used as a binary indicator of a location existing in dryland or mesic environment, we do not expect use of GPM MAP estimates at these four sites to bias results. We also used International Geosphere-Biosphere Program (IGBP) land cover classification information to broadly assess vegetation types (Kim, 2013). Finally, we used fraction of vegetation cover as converted from MODIS leaf area index to assess vegetation presence in drier climates in our study region (Myneni et al., 2015).

2.2. Data Set Representation

While different in their representation, NEP and VOD are complementary whole-canopy, large spatial scale metrics that may be sensitive to rain pulses. Both NEP and VOD are integrated metrics of different components of plant behavior. NEP equals GPP minus R_e, where GPP represents photosynthesis via the rate of ecosystem CO_2 uptake and R_e represents ecosystem CO_2 effluxes due to both heterotrophic (i.e., soil microbes) and autotrophic processes (Law et al., 2002). VOD, linearly proportional to plant water content, is influenced by both structural growth/decay (creating more/less water storage space) and relative water content (water uptake/loss independent of growth) (Konings et al., 2019; Momen et al., 2017; Tian et al., 2018; Zhang et al., 2019). These metrics are complementary in that NEP and VOD may observe different components of daily vegetation use of rain pulses, such as plant hydraulic (i.e., rehydration) and photosynthetic responses (i.e., carbon assimilation). Note that our primary analysis refrains from partitioning NEP and VOD into more fundamental components to avoid model assumptions that may prescribe (either explicitly or implicitly) pulse behavior we attempt to estimate. Finally, both metrics are integrated over large spatial scales allowing evaluation of behavior beyond individual species. NEP integrates ecosystem carbon flux behavior at 100-m scales, while SMAP VOD observations integrate plant water content at landscape scales of tens of kilometers.

The inherent spatial sampling and time domain differences between NEP and VOD pose a limitation in their joint analysis. Specifically, VOD will observe a larger area of vegetation than that of NEP at a given site. Additionally, their time domains do not overlap, hindering direct comparison of specific events between data sets. It is, therefore, assumed that the pulse responses do not change over the time domain covered here (1995–2019). The validity of this assumption is uncertain given limited characterization of pulse responses. Pulse-response magnitudes and timing may shift with processes such as land cover change, climatic change, and interannual weather and climate variability. For example, free-air carbon dioxide enrichment experiments show that increased ambient carbon dioxide concentrations can alter stomatal responses and thus the magnitude of the NEP response over decade-long durations (Ainsworth & Long, 2005; Bernacchi et al., 2007). These leaf gas exchange magnitudes can be further influenced by increases in vapor pressure deficit (VPD) with temperature (Novick et al., 2016). Further assessment of this stationary pulse-response assumption is beyond the scope of this study. Ultimately, rather than directly compare the two metrics, we intend to assess gradients in NEP and VOD behavior between dryland and mesic environments and their responses to varying pulse characteristics.
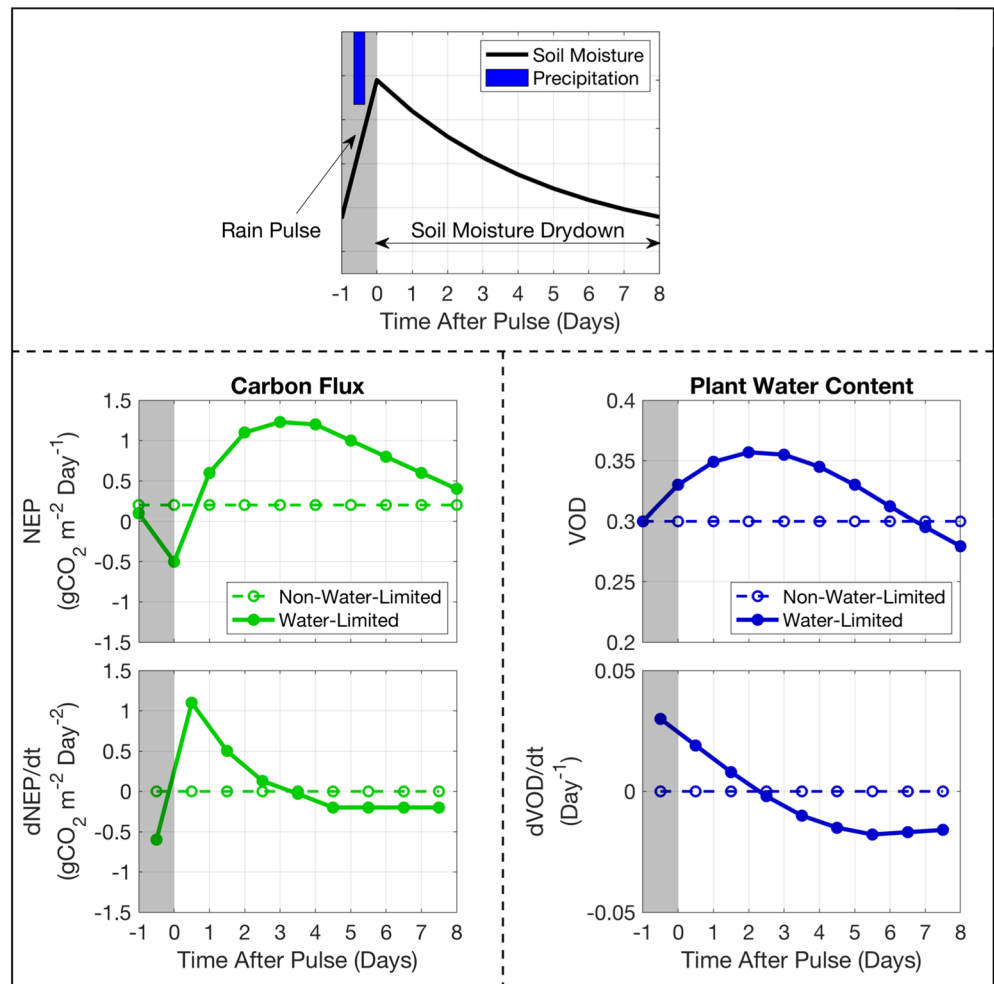
Figure 1. Conceptual soil moisture pulse and expected photosynthetic and hydraulic responses for water-limited and non-water-limited ecosystems. Expected responses are shown for variables used in this study: flux tower observed net ecosystem production (NEP) and satellite-observed vegetation optical depth (VOD, proportional to plant water content). Non-water-limited ecosystem responses represent no detectable NEP or VOD response. Gray shading indicates the rain pulse period when soil moisture is increasing (before day 0). The nonshaded region is the interpulse period when the soil moisture drydown occurs (after day 0). dNEP/dt and dVOD/dt values are reported with the convention that the change rate between 0 and 1 day after pulse is reported between the 2 days or 0.5 days after the pulse.

2.3. Pulse Period Identification

We identified rain pulses using the surface soil moisture time series from both field and satellite observations. Given that rain pulses produce concurrent soil moisture pulses, both terms are used synonymously throughout this study. A conceptual soil moisture pulse is shown in Figure 1. Use of soil moisture rather than precipitation to identify pulses is recommended because soil moisture is more ecologically relevant to plants and it integrates temporal storm details (Reynolds et al., 2004). Furthermore, use of the shallow soil moisture layer to identify pulses and their characteristics is an advantage for this application because this layer will respond to nearly any rain size pulse, unlike deeper soil layers (Kurc & Small, 2007; Schwinning et al., 2003; Scott et al., 2006). Specifically, a pulse period, or soil moisture drydown, is defined here as a detectable signal of volumetric soil moisture increase (>0.01 m^3/m^3) followed by at least four consecutive measurements of soil drying (McColl et al., 2017). Four consecutive measurements were chosen to filter out short drydowns falsely detected due to noise. Due to sampling frequency differences between data sets, this definition results in drydowns of at least 4 days for flux tower observations and at least 6–8 days for satellite observations. The difference in drydown identification length is not expected to impact results because

responses are typically detected here in the first 3 days of the drydown. SMAP 9 km data were pooled within half degree pixels to increase drydown samples. Note that small subsequent rain events may have occurred during the identified drydowns but were ultimately too small in magnitude to discontinue soil drying and were thus likely negligible compared to the initial pulse.

2.4. Pulse-Response Assessment

Figure 1 conceptually displays our expectations of NEP and VOD pulse responses for the driest and most humid ecosystems. Specifically, ecosystems with sufficiently available water may nominally exhibit no tendency to change NEP or VOD following a rain pulse with variability instead due to temperature, light, and nutrients ("non-water-limited" case in Figure 1). Conversely, a rain pulse may cause distinct hydraulic and photosynthetic responses as seen by NEP and VOD in dryland ecosystems ("water-limited" case in Figure 1). Increases in NEP can indicate primary production responses where carbon uptake accelerates above that of prestorm conditions. This may follow an immediate NEP decrease due to upregulation of respiration. This respiration response is known as the "Birch effect" where rewetting of previously dry conditions activates soil microbes, releasing soil carbon through decomposition processes (Jarvis et al., 2007). VOD can detect water uptake and pulse-driven growth responses, with the time scale of water uptake depending on the plant's capacitance and resistances (Phillips et al., 2004). In the absence of dry biomass changes on these time scales, 6 a.m. observed VOD may represent predawn water potential (i.e., xylem and leaf). Since soil and plant (xylem, leaf, etc.) water potentials are commonly thought to approach equilibrium overnight (Donovan et al., 2001), nominal rapid rehydration responses following rainfall may result in VOD closely covarying with soil moisture. Beyond nominal rehydration responses, we suspect that the driest ecosystems may frequently show multiday VOD responses to rain pulses due to pulse-driven growth and/or slow rehydration due to hydraulic recovery upon rewetting (such as recovering soil–root interface) (Blackman et al., 2009; Carminati et al., 2017; Noy-Meir, 1973). Therefore, both NEP and VOD upregulation responses in drylands are expected to occur over multiple days after rewetting of drier soil conditions. We anticipate that both NEP and VOD will eventually decrease with drying soil with decelerating carbon uptake and plant water loss. Our procedure here evaluates these expectations.

NEP and VOD immediately preceding and during these drydown periods (before and during the storm) were recorded. With the goal of isolating plant responses due to the rain event alone, the seasonal cycles were subtracted from the NEP and VOD time series to remove confounding effects (i.e., seasonal phenology) according to Feldman et al. (2019). Additionally, the first difference (derivative) was taken of the NEP and VOD time series to remove dependence on absolute NEP and VOD values, highly coupled to climatology. The resulting $dNEP/dt$ and $dVOD/dt$ metrics allow closer evaluation of daily to weekly plant responses to individual rain pulses. A conceptual time series of NEP and VOD with conversion from absolute units to the first difference for both NEP and VOD is shown in Figure 1. $dNEP/dt$ becomes an acceleration which measures the ability for the ecosystem to upregulate, as was used previously to evaluate soil respiration (Potts et al., 2014). $dNEP/dt$ and $dVOD/dt$ values from all drydowns at each (later specified) site were binned based on the day after the start of the drydown. Note the caveat that sites with more identified drydowns, due in part to longer records, will influence the aggregated NEP behavior more (Table 1).

To evaluate the frequency of upregulation responses as observed by both data sets, the fraction of pulses with NEP and VOD increases on the first day following the pulse was computed at each location. This metric assesses how frequently NEP and VOD increase rather than decrease on the day following the rain pulse. It serves as an indicator for frequency of poststorm lagged hydraulic, photosynthetic, and growth responses, suggesting upregulation from previously dry soil conditions. This comparison serves to set the stage for more detailed analyses that follow.

2.5. Pulse Characteristic Assessment

To evaluate the effects of pulse characteristics, the pulse magnitude and antecedent soil moisture were recorded for each drydown period. The pulse magnitude is defined as soil moisture at the beginning of a drydown minus soil moisture before the drydown. The antecedent soil moisture is defined as the soil moisture value before the drydown beginning. Within a site, each drydown was binned into small/large pulse mag-

nitude and dry/wet antecedent moisture conditions based on whether the pulse characteristics are above or below the median of the respective condition. These classifications result in four combinations of pulse characteristics (small or large pulse magnitude and dry or wet antecedent moisture). Results are insensitive to bin thresholds; nearly identical results are obtained when binning below the 40th percentile and above the 60th percentile of the respective pulse characteristic. Surface soil moisture may not be characteristic of the rootzone conditions if deeper rooting distributions exist, which may impact validity of antecedent moisture definitions here. However, daily-scale surface soil moisture has been shown to be correlated with deeper soil layer moisture variations, especially in mesic environments (Short Gianotti, Salvucci, et al., 2019).

Kruskal–Wallis nonparametric tests were performed to determine whether there are significant differences ($p < 0.05$) in medians of the four pulse scenario distributions (combinations of small/large pulse magnitude and dry/wet antecedent moisture) on each day after the pulse. This was completed for both NEP and VOD.

2.6. Response Uncertainty Assessment

We created a null model to determine whether the dVOD/dt or dNEP/dt values are significantly different from that of a random noise series that is purposefully independent of soil moisture (where mean variable change rates are zero). Specifically, the null model tests whether the NEP and VOD behavior is different from that of the "non-water-limited" scenario in Figure 1. For each location, we generated a random NEP time series with the same mean, variance, and first-lag autoregressive coefficient as the original NEP time series. One hundred NEP time series replicates were created. These synthetic dNEP/dt series were also binned based on the day after the pulse coinciding with the observed soil moisture drydowns. Mann–Whitney U tests were performed between the synthetic and observed dNEP/dt distributions to assess whether the dNEP/dt values on that day after the pulse are significantly different from random noise with median zero ($p < 0.05$). Significance indicates dNEP/dt values depend on soil moisture on the respective day. This procedure was repeated for VOD.

2.7. Moisture Threshold Detection

To determine if soil moisture state-dependence behavior exists, we assessed dNEP/dt and dVOD/dt behavior versus soil moisture at each site. We specifically divided the dNEP/dt values into two bins above and below a given soil moisture threshold, based on the soil moisture values that the dNEP/dt values cooccurred with. We then tested whether the difference in the two dNEP/dt distributions is statistically significant. A tested soil moisture value was labeled a significant threshold if the dNEP/dt median above this moisture value is both (1) significantly greater than zero (Mann–Whitney U test between dNEP/dt observations and dNEP/dt null model distribution; $p < 0.05$) and (2) significantly greater than the dNEP/dt distribution median below this moisture value (Mann–Whitney U test between dNEP/dt medians at high and low soil moisture; $p < 0.05$). Together, these criteria determine whether wetter soils show stronger increases in carbon uptake than do drier soils. We tested soil moisture values in 0.01 m^3/m^3 intervals between the maximum and minimum soil moisture value at each site and computed the fraction of successful detections out of the total number of soil moisture values tested. A higher value of this metric will suggest nonlinear NEP and VOD behavior indicative of moisture threshold behavior at the respective site. This same process was repeated for dVOD/dt to determine whether wetter soils result in greater dVOD/dt. These criteria are robust to nonlinear and seasonal relationships with soil moisture. Based on 5 cm surface soil moisture holding information about moisture from deeper soil layers, we anticipate that the detected threshold represents nonlinear soil moisture behavior from deeper than 5 cm (Short Gianotti, Salvucci, et al., 2019).

3. Results and Discussion

3.1. Gradient of Pulse Responses

We find that vegetation in drier environments tends to show more frequent poststorm upregulation responses, where NEP and VOD tend to increase on the first day after the rain pulse (Figure 2). This
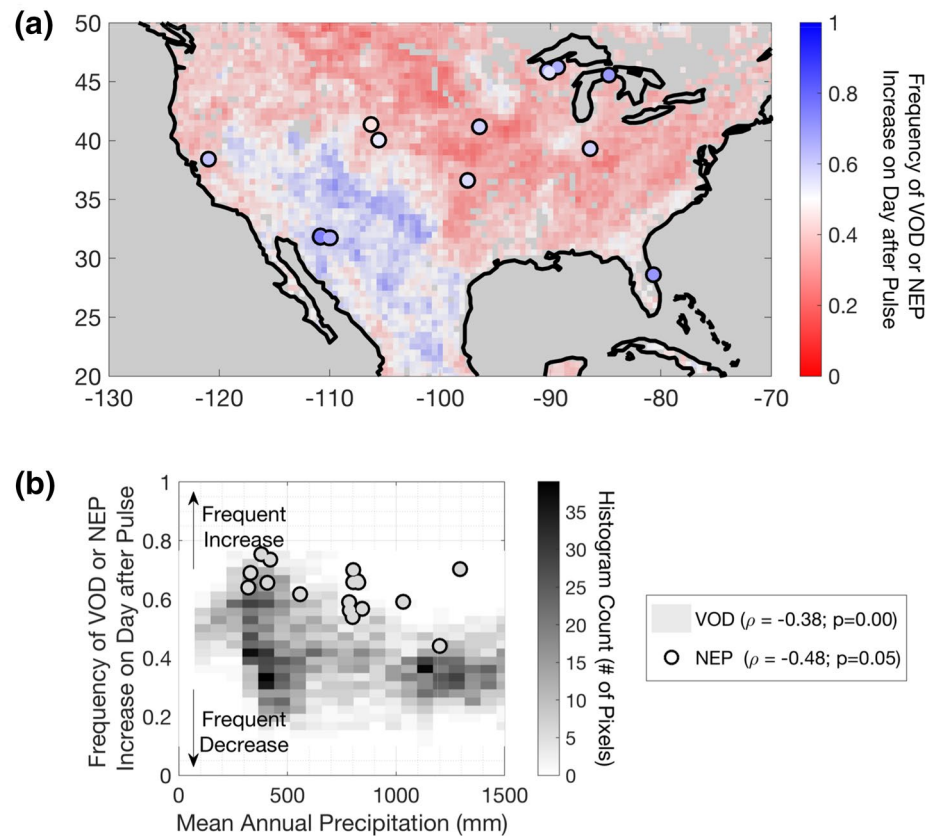
Figure 2. Frequency of satellite-observed vegetation optical depth (VOD, proportional to plant water content; shading) and flux tower observed net ecosystem production (NEP; symbols) increases on the first day of soil drying after rainfall. (a) Spatial pattern. (b) Joint density of all observations in (a) versus observed mean annual precipitation. Fractions above 0.5 indicate a tendency for NEP or VOD to increase (indicating photosynthetic and/or hydraulic upregulation responses following previously drier soil conditions; see text) on the first day of soil drying following the rain event. Fractions below 0.5 indicate a tendency for NEP or VOD to decrease since one minus the fraction indicates the frequency of decrease. Only sites with sufficient drydown samples to generate metric ($N > 30$) are shown here.

is shown with negative correlations between increase frequencies (for both NEP and VOD) and MAP ($p < 0.05$; Figure 2b). For NEP, this negative correlation with the rainfall gradient is more apparent considering only the sites across the Southwest US to Midwestern US grasslands with convective rainfall regimes ($\rho = -0.87$; $p < 0.01$). While NEP tends to increase across the United States after rainfall (fractions > 0.5), increases are more prevalent in drylands. VOD tends to increase after rainfall across the Southwest US drylands but tends to decrease across the mesic Midwestern and Eastern United States. These results are for the continental US spring and summer months. The gradient of behavior for NEP disappears in the winter months due to reduced pulse responses in drylands and increased responses in Mediterranean climates along the US west coast (Figure S2). We focus only on spring and summer months for the remainder of our analysis.

NEP variations likely reflect GPP rather than R_e variations here. NEP (or GPP-R_e) could increase due to GPP increases, R_e decreases, and/or GPP increasing more than R_e is. Results repeated with FLUX-NET-partitioned GPP show nearly identical results (not shown). Furthermore, previous field studies show that R_e tends to increase which would instead decrease NEP immediately after a rain event due to the "Birch effect" (Chen et al., 2009; Huxman, Cable, et al., 2004; Jenerette et al., 2008; Roby et al., 2020; Williams et al., 2009; Xu et al., 2004). Therefore, we interpret the frequent NEP increases as GPP upregulation. Fractions greater than 0.5 are thus interpreted as photosynthetic activity consistently accelerating above prestorm levels after rainfall. Partitioning GPP and R_e is discussed further in Section 3.2.

VOD tends to increase after the pulse in the Southwest US drylands indicating canopy upregulation through growth and/or slow rehydration. Based on VOD's proportionality to vegetation water content, positive dVOD/dt after rain pulses can represent a growth response and/or multiday predawn water potential rehydration due to hydraulic recovery from dry conditions. Consistent with our findings, growth responses on daily to weekly scales (Angert et al., 2007; Miao & Bazzaz, 1990; Novoplansky & Goldberg, 2001; Ogle & Reynolds, 2004; Post & Knapp, 2019; Sher et al., 2004) as well as multiday plant water storage increases under dry initial conditions have been observed across drylands previously (Blackman et al., 2009; Brodribb & Cochard, 2009; Fravolini et al., 2005; Ignace et al., 2007; West et al., 2007).

Vegetation in the more humid US regions still shows discernable sensitivity to rain pulses despite showing less frequent upregulation. NEP in the mostly mesic Midwestern and Eastern US regions shows a subdued tendency to increase with values over 0.5. VOD shows more frequent decreases after rain pulses in these regions, suggesting frequent water loss, indicated as values below 0.5 (red shading in Figure 2a). We suspect that the decreased pulse-response frequency is primarily because these mesic regions are limited by other resources (such as light, temperature, and nutrients) where pulsed water inputs only marginally increase ecosystem photosynthesis from its current state (Short Gianotti, Rigden, et al., 2019). Additionally, frequent VOD decreases likely indicate maintenance of predawn water potential equilibrium during soil drying where upregulation is less frequent (see Section 3.2). Nevertheless, rain pulses still appear to influence these more humid ecosystems.

It is unclear why only dryland vegetation in the Southwest United States exhibits multiday increases in plant water content after rain pulses. Portions of the Great Plains grasslands, while also receiving low amounts of rainfall (<500 mm/year), tend to instead show rapid decreases in plant water content during soil drying after rainfall (Figure 2b, fractions < 0.5 in drier environments). These regions also tend to show infrequent VOD increases during the pulse indicating that no rehydration is occurring (not shown). IGBP land cover classifications show that these two regions are divided by broadly differing vegetation types with shrublands in the Southwest United States and grasslands across the Great Plains. These differing responses suggest more opportunistic pulse water usage of the summer convective events for Southwest US vegetation as opposed to usage of summer events across the Great Plains, potentially related to the regions' differing phenologies.

Despite low vegetation coverage in the Southwest United States, VOD observations are likely detecting vegetation variability not due to artifacts. Both fraction of vegetation cover and mean VOD, an indicator of aboveground dry biomass (Brandt et al., 2018), show that the Southwest US shrublands have a detectable vegetation presence similarly to the Midwest US grasslands (Figure S3). These values are statistically significantly different than that of baseline nonvegetated surfaces (with the Sahara desert used as a test) which expectedly show near-zero mean VOD and do not return vegetation fraction values (due to soil contamination in the visible and near-infrared spectrums).

3.2. Dryland and Mesic Environment Comparison

The summary metric in Figure 2 provides information only on VOD and NEP changes on the first day after the rain pulse ignoring behavior during the pulse and possible further lagged behavior (Ogle & Reynolds, 2004; Williams et al., 2009). This limitation motivates evaluating the full-time evolution of behavior during drydowns in each region. Due to a potential trend in NEP and VOD behavior from dryland to mesic regions, there may also be differences in pulse behavior between these environments. Additionally, far less is known about pulse behavior in mesic than dryland environments. We therefore aggregate mesic and dryland sites separately for comparison. These regions are partitioned based on a 500-mm MAP threshold below which regions are typically classified as arid to semiarid (Noy-Meir, 1973). Note that results are not qualitatively sensitive to this arbitrary MAP threshold selection. We analogously evaluate SMAP VOD for the pixels that contain each tower site.

In drylands, we find that the frequent poststorm VOD and NEP increases observed in Figure 2 continue typically for 2–3 days into soil moisture drydowns with weaker increases after the first day (Figures 3a
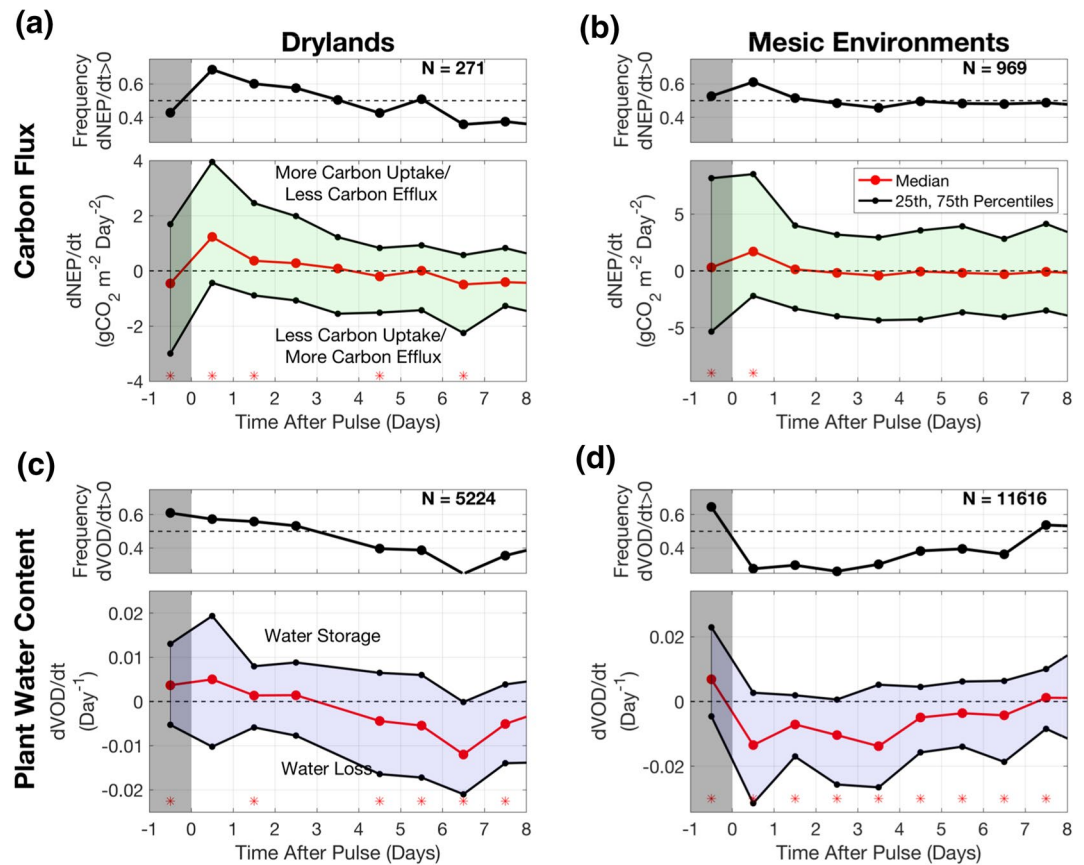
Figure 3. Carbon flux (NEP) and plant water content (VOD) behavior aggregated across all dryland and mesic sites in Table 1 on each day after rain pulses. (a) NEP drylands. (b) NEP mesic environments. (c) VOD drylands. (d) VOD mesic environments. Soil moisture increases during the pulse in the shaded gray region (before day 0) and decreases thereafter (see Figure 1). For consistency, only VOD pixels nearest to each FLUXNET site were used. dNEP/dt and dVOD/dt values are reported with the convention that the change rate between 0 and 1 day after pulse is reported between the 2 days or 0.5 days after the pulse (see Figure 1). N is the total number of drydown samples from all sites in the respective panel. Since pulse samples are disproportionate across FLUXNET sites (Table 1), VOD distributions are weighted using a resampling technique to ensure that a given site contributes proportionally to both NEP and VOD distributions while preserving the original sample size. y axis limits are adjusted based on NEP and VOD standard deviations to proportionally compare dryland and mesic environment change rates (right and left columns). The red asterisk indicates that the change rate has a statistically significant response to the rain pulse on the respective day (Mann–Whitney U test between null model and distribution; $p < 0.05$). The frequency metric in the top panel is the same as that reported in Figure 2. Refer to Table 1 and Figure S1 for site information. NEP, net ecosystem production; VOD, vegetation optical depth.

and 3c). Dryland NEP exhibits significant, frequent NEP increases over the first 2 days of the drydown after a 1-day delay and decreases after 5 days of soil drying (Figure 3a). VOD shows similar dynamics albeit with increases beginning during the rain pulse (Figure 3c). This time evolution suggests that the NEP and VOD peaks generally occur between 2 and 4 days after the pulse (Figure 1). The NEP behavior shows photosynthetic rates consistently increasing above prestorm levels and eventual decreases given sufficient drying between storms. This behavior is broadly consistent with previously measured NEP behavior at similar dryland sites (Chen et al., 2009; Q. Guo et al., 2016; Y. Hao et al., 2010; Loik, 2007; Scott et al., 2006; Tang et al., 2018). Note that longer durations of NEP and GPP increases have been observed previously (Kurc & Small, 2007; Williams et al., 2009). The VOD behavior shows that slow rehydration and/or pulse-initiated growth begins during the rain pulse and typically continues for multiple days. Partitioning these aforementioned VOD phenomena is beyond the scope of this study, but we conjecture about them in Section 3.3.1.
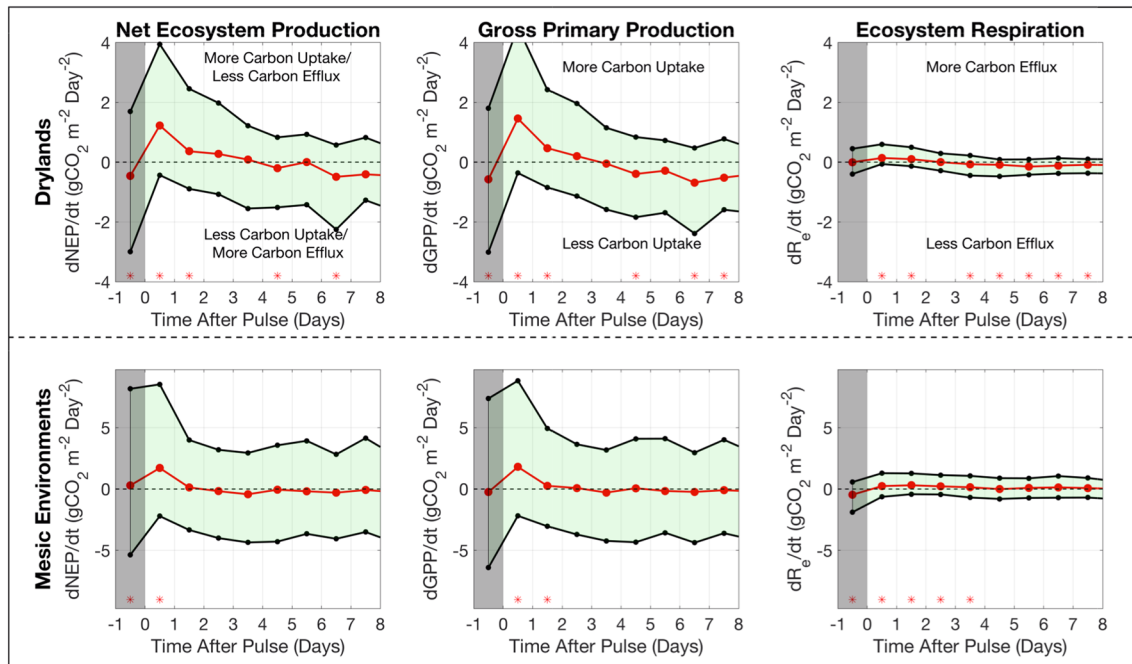
Figure 4. Partitioned carbon flux behavior following rain pulses. FLUXNET-modeled estimates of NEP partitioned into GPP and R_e. Same labeling as Figures 3a and 3b. NEP, net ecosystem production; GPP, gross primary production.

Contrary to our expectations, mesic US vegetation is sensitive to pulses with a brief period of primary production increases and plant water content behavior indicative of rapid rehydration and drying under predawn equilibrium. NEP increases in mesic environments, though with less frequency and with no significant changes persisting for more than a day (Figures 2 and 3b). Since drying continues uninterrupted for at least 4 days in the selected drydown periods, it is unlikely that shorter NEP responses are an artifact of more frequent rainfall in mesic environments. VOD frequently increases rapidly during the pulse period, followed by sustained frequent drying in step with soil moisture during the drydown (Figure 3d). These 6 a.m. observed VOD dynamics likely represent predawn water potential equilibration with soil water potential, with plants rehydrating during the rain pulse then drying in step with soil moisture during the drydown. This interpretation is based on the assumption of minimal dry biomass changes during the drydown and widespread near-linear, monotonic relationships between relative water content and plant water potential (Konings et al., 2019). Interception may also contribute to the initial VOD increase. We suspect that the consistent VOD decreases during drydowns are due to water content loss (i.e., transpiration) rather than structural decay (i.e., leaf-off and mortality). Despite consistent plant water content and soil drying, NEP does not decrease (or downregulate), suggesting carbon uptake dynamics do not typically reach a water-limited state at least initially under a week of continued drying (Figures 3b and 3d). This NEP and VOD behavior ultimately further supports that mesic environment vegetation responds to pulses, though with more subdued behavior compared to dryland environments. It is possible that the most humid environments (such as tropical rainforests), which receive more than twice the rainfall of the humid environments in the United States, may show no responses as in Figure 1.

Poststorm NEP increases are likely due primarily to increases in GPP with only small changes in R_e. Two lines of evidence using FLUXNET-modeled separation of NEP into GPP and R_e and nighttime carbon fluxes suggest that R_e fluctuations are comparatively smaller on this time scale in our study. First, GPP and R_e-partitioned estimates show that R_e changes are comparably smaller (~15% of GPP) and therefore NEP primarily represents GPP behavior (Figure 4). Second, nighttime (12 a.m.–6 a.m.) NEP behavior also suggests that R_e changes are relatively smaller (~30% of daytime NEP; Figure S4). Overnight carbon fluxes are thought to reflect R_e behavior (Jenerette et al., 2008; Kurc & Small, 2007), though see Fisher et al. (2007) for uncertainties due to active nighttime transpiration. The two methods show different timing of R_e increases
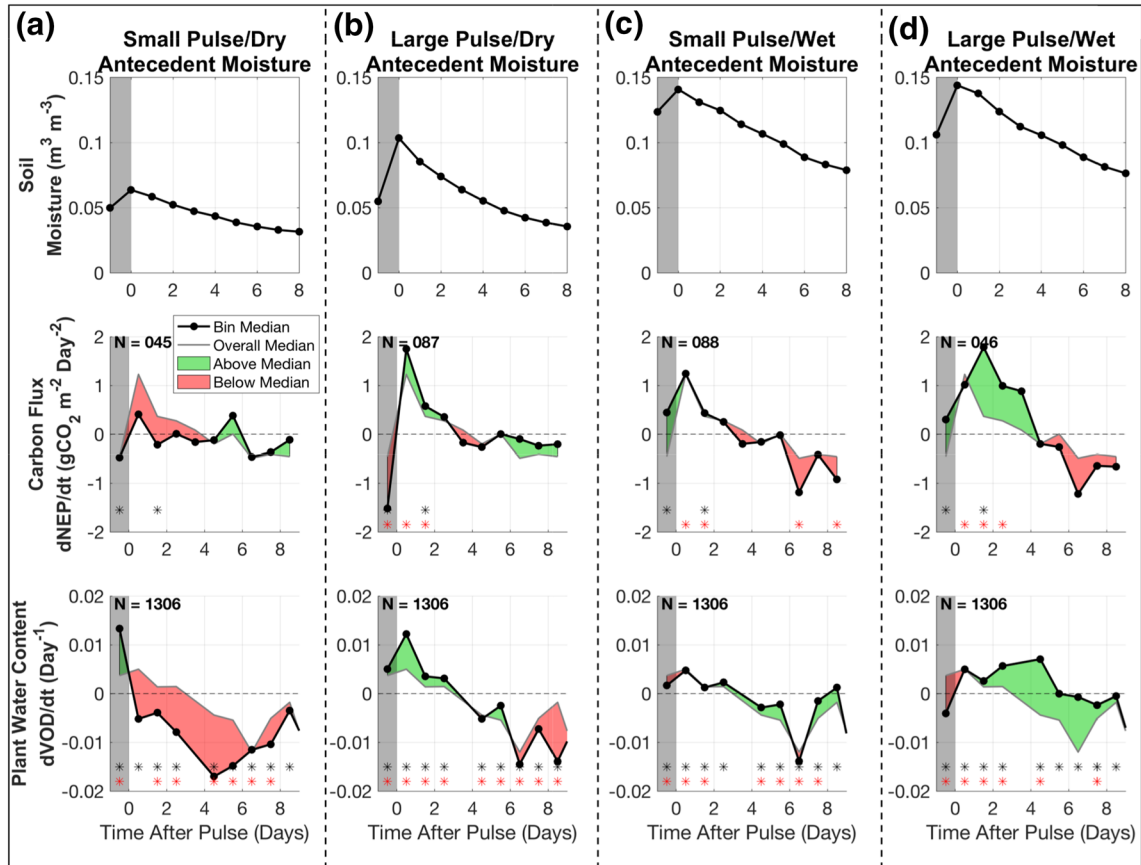
Figure 5. Dryland ecosystem (MAP < 500 mm/year) carbon flux (NEP) and plant water content (VOD) behavior following pulses binned based on pulse size and antecedent soil moisture conditions (a–d). (a) Small pulse, dry antecedent soil moisture. (b) Large pulse, dry antecedent soil moisture. (c) Small pulse, wet antecedent soil moisture. (d) Large pulse, wet antecedent soil moisture. The median FLUXNET soil moisture time series in each bin is reported in the top row for reference though noting satellite soil moisture was used to bin the VOD responses. The "overall median" is reproduced from Figure 3 as a gray line and is the same across all bins. The "bin median" is the median for its respective bin shown in the bold line. Colored shading indicates that the bin median is above (green) or below (red) the overall median from Figure 3. N indicates the number of pulses in each bin. A black asterisk indicates that the Kruskal–Wallis test shows significantly different distributions in rates of change between the four pulse cases for a given day ($p < 0.05$). The red asterisk indicates that the change rate has a statistically significant response to the rain pulse on the respective day (Mann–Whitney U test between null model and distribution; $p < 0.05$). Refer to Table 1 and Figure S1 for site information. NEP, net ecosystem production; VOD, vapor pressure deficit.

with nighttime NEP suggesting they begin during the storm and FLUXNET-partitioned estimates showing R_e increases on the day after the storm (Figures 4 and S4). Nevertheless, previous studies instead show larger R_e increases within the day after rainfall that may overwhelm the initial GPP response (Huxman, Cable, et al., 2004; Jenerette et al., 2008; Kurc & Small, 2007; Potts et al., 2006). We suspect that the smaller R_e changes here are due to evaluating pulse behavior during spring and summer months when soil microbes have already largely upregulated following dormancy during the winter months. We ultimately interpret the NEP increases to be due to primary production as seen in previous studies (Roby et al., 2020), though with caution considering uncertainties in partitioning GPP and R_e and using nighttime carbon fluxes.

3.3. Dependence of Pulse Responses on Pulse Characteristics

We find that varying pulse characteristics, specifically antecedent moisture conditions and pulse magnitudes, results in significantly different NEP and VOD responses in drylands but has little effect on responses in mesic environments (Figures 5 and 6). Linear regressions between pulse characteristics and NEP and VOD rates of change agree with the direction of tendencies in Figures 5 and 6 (see Figures S5 and S6). These results are thus robust to the binning methods applied in Figures 5 and 6. Therefore, given that previous studies identified pulse moisture thresholds and effects of antecedent soil moisture, plotting all pulse
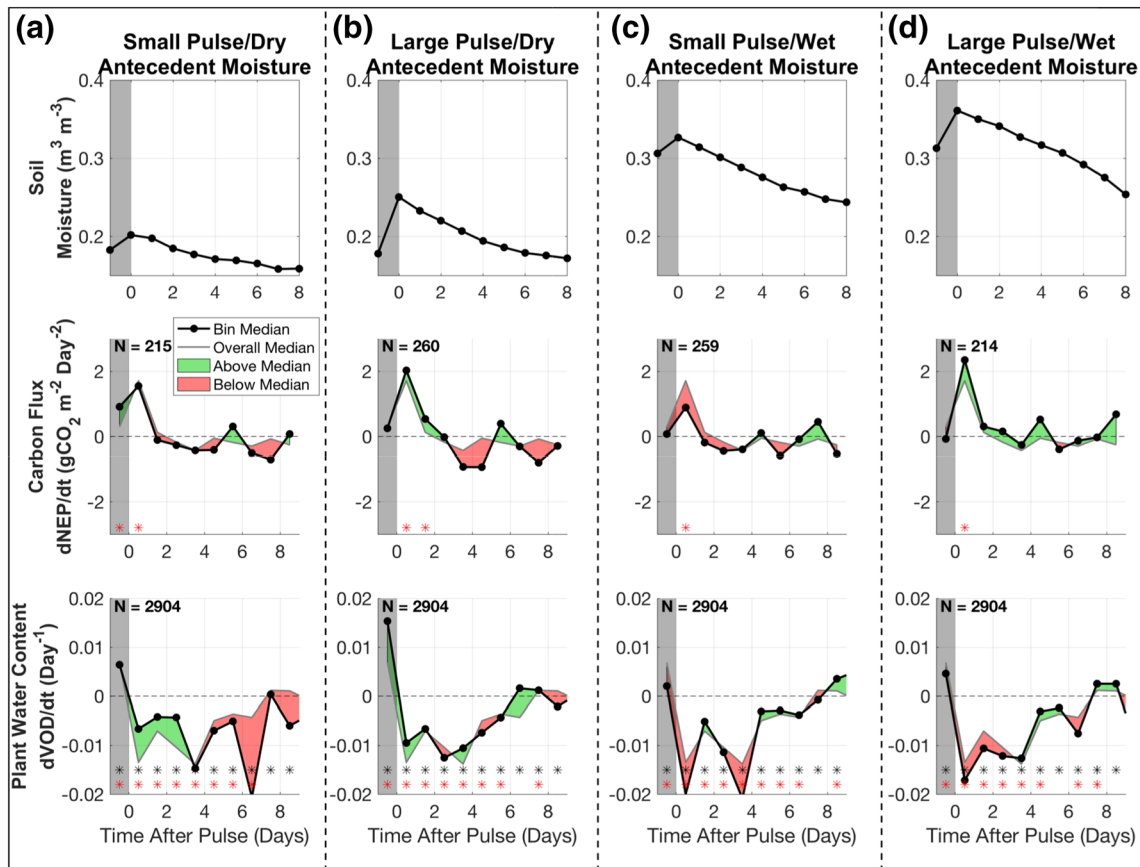
Figure 6. Mesic ecosystem (MAP ≥ 500 mm/year) carbon flux (NEP) and plant water content (VOD) behavior following pulses binned based on pulse size and antecedent soil moisture conditions. The notation and format are the same as Figure 5. NEP, net ecosystem production; VOD, vapor pressure deficit.

behavior in Figure 3 appears to obscure dependence on these characteristics at least in drier environments (Feldman et al., 2018; Potts et al., 2006; Reynolds et al., 2004; Schwinning et al., 2004).

3.3.1. Drylands

Following smaller pulses under initially dry soil, no consistent carbon flux change occurs and plant water content consistently dries along with soil moisture (Figure 5a). Initial increases in VOD occur during the pulse suggesting a rehydration response. However, VOD dries consistently with soil moisture loss and no changes in carbon uptake are exhibited. These responses may indicate that the soil rewetting event was insufficient to create a significant photosynthetic response. We discuss this scenario further in the context of thresholds in Section 3.3.3.

Following larger pulses on initially dry soil, NEP increases occur with a lag beginning during the first day of soil drying, due likely to a delay in GPP upregulation (Figure 5b). The initial decrease in NEP may be because of a combination of increased respiration from rewetted soil microbes (Jenerette et al., 2008; Xu et al., 2004) and continued GPP loss during the previous interpulse period as supported by nighttime carbon fluxes and partitioned flux estimates (Figure S7b). The 1-day lagged NEP increase appears to be due to a GPP increase, though its magnitude and duration of increase is less than when the soil is initially wetter as is consistent with previous findings (Potts et al., 2006). Additionally, VOD shows consecutive increases during and following the pulse with a similar delayed larger increase the day following the pulse (Figure 5b). With drier initial soil conditions, these consecutive plant water content increases may in part represent slow rehydration due to previously dry conditions that may have created initially high soil–plant resistances

(such as from soil–root disconnection and xylem cavitation) (Carminati et al., 2010; Lo Gullo et al., 1998; North & Nobel, 1991, 1997; Trifilò et al., 2004; West et al., 2007).

Following smaller pulses on initially wet soil, NEP increases are subdued (with insignificant increases; $p < 0.05$) but occur immediately during the storm rather than with a day delay (Figure 5c). Based on partitioned estimates and nighttime fluxes, no respiration response occurs perhaps because of initially wetter conditions (Figure S7c). Similarly, plant water content increases are weaker (Figure 5c). This similar initial VOD and NEP behavior indicates that wetter initial moisture conditions create quicker responses due to previous upregulation, but more intense rainfall may be required for a discernable response to be exhibited.

Following larger pulses on initially wet soils, dryland NEP and VOD exhibit the longest and greatest increases (Figure 5d; bin median is above overall median). Larger pulses enhance VOD and NEP increases beyond the second day of the drydown (Figures S5 and S6). These longer VOD increases are potentially detecting rainfall-triggered dry biomass growth based on several lines of reasoning. First, the gradual VOD increases are not likely due to slow rehydration because hydraulic conductivities throughout the soil–plant continuum (including soil–root interface and xylem) are typically highest under initially wet conditions (Lo Gullo et al., 1998; Martorell et al., 2014; North & Nobel, 1997; Trifilò et al., 2004). Second, rapid growth requires high cell turgor with the help of wet soil as is the case under these conditions (Kramer & Boyer, 1995). Third, the longest duration carbon flux increases (likely from increases in GPP; Figure 4) are concurrent with these consecutive VOD increases reflecting rapidly upregulating and continued photosynthetic processes (Figure 5d). Week-long growth responses to larger pulses have been detected in drylands previously (Post & Knapp, 2019). Furthermore, studies also found that primary production is of greater magnitude and longer duration following larger pulses on wetter antecedent moisture (Chen et al., 2009; Loik, 2007; Plaut et al., 2013; Tang et al., 2018). These observations therefore provide evidence for pulsed growth as hypothesized under the pulse-reserve paradigm (Noy-Meir, 1973).

3.3.2. Mesic Environments

While plants in mesic environments on average tend to respond to pulses, different pulse conditions greatly influence neither their carbon flux responses nor their plant water content responses (Figures 3 and 6). There are no significant differences between pulse characteristics in carbon flux behavior (Figure 6, middle row; $p < 0.05$). VOD changes similarly show nearly identical magnitudes and signs of responses across all bins of pulse characteristics (Figure 6, bottom row). Statistical significance is likely inflated by the large VOD sample size here.

It is well known from remote sensing and field studies that vegetation in humid regions, especially in the temperate Eastern United States, shows greater sensitivity to temperature and light than soil moisture variability (Madani et al., 2017; Nemani et al., 2003). This is in part because these more humid regions exist in an energy-limited state where soil water availability has less influence on evapotranspiration and GPP (Akbar et al., 2018; Koster et al., 2009; Short Gianotti, Rigden, et al., 2019). Given that there is still a vegetation response to pulses, but no response sensitivity to soil moisture pulse characteristics, pulse-response variability may be a greater function of other variables' dynamics. Temperature, VPD, and incoming solar radiation can increase on the scale of drydowns (Feldman et al., 2019). It has also been shown that VPD influences leaf gas exchange more in mesic environments (Novick et al., 2016). Additionally, nutrient availability during wetting and drying cycles can be variable based on soil microbe behavior (Gessler et al., 2017; Jarvis et al., 2007). We suspect that initial conditions of these aforementioned variables and their dynamics over a drydown may instead control differences in mesic vegetation pulse responses. Evaluation of these other environmental factors is beyond the scope of this work.

3.3.3. Soil Moisture Threshold Detection

We find that satellite VOD and flux tower NEP show soil moisture threshold behavior in drylands but less so in mesic regions (Figure 7). This difference in part explains why dryland vegetation shows no NEP changes and consistent plant drying under small pulse and dry initial conditions, while NEP and VOD increase
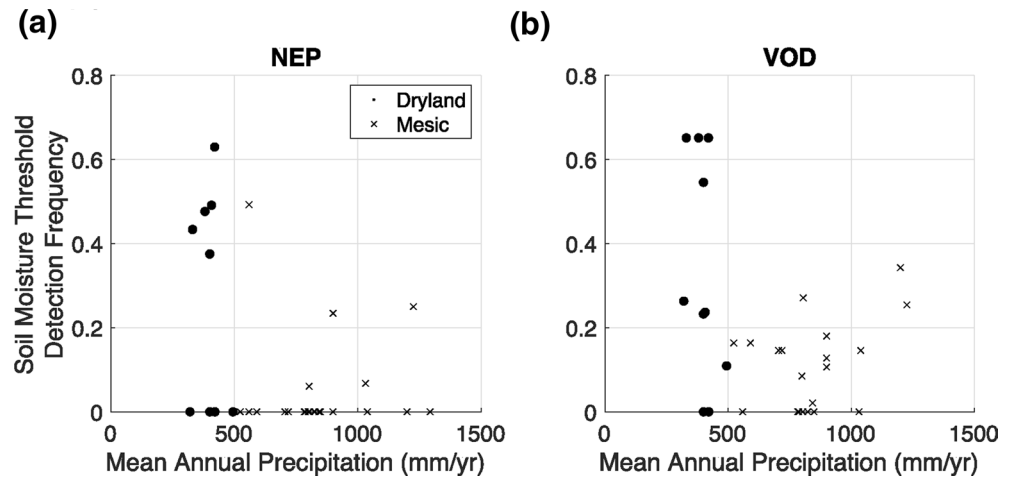
Figure 7. Soil moisture threshold detection frequency at each site. Fraction of tested soil moisture values that suggest significant moisture threshold behavior for (a) NEP and (b) VOD ($p < 0.05$) at each site. Higher fraction values suggest more confidence in threshold detection. At a given site, a successful moisture threshold detection requires the dNEP/dt (or dVOD/dt) median at high soil moisture to be significantly greater than zero and greater than the median at low soil moisture ($p < 0.05$; see Section 2.7). NEP, net ecosystem production; VOD, vapor pressure deficit.

under well-watered conditions (Figure 5). Water-limitation may induce dormancy conditions, perhaps even intermittently between rainfall within a rainy season, where plants on average upregulate above basal photosynthetic activity only when rootzone moisture is increased to sufficiently wet conditions (Knapp et al., 2008; Schwinning & Sala, 2004). Conversely, moisture thresholds appear less prevalent in mesic environments, where carbon and water uptake responses occur following both small and large pulses regardless of antecedent moisture conditions (Figure 6). Moisture thresholds may still exist in mesic environments, but the land surface may only infrequently dry to states where moisture pulses are no longer ecologically important. Instead, temperature, humidity, nutrient, or radiation thresholds may more commonly control these environments (Jarvis, 1976).

Threshold behavior has been detected previously in semiarid environments, though primarily using rain depth (Chen et al., 2009; Y. Hao et al., 2010; Sala & Lauenroth, 1982; Tang et al., 2018). Use of soil moisture is preferred here because it holds more information about initial moisture conditions (Reynolds et al., 2004). Consistent with results here, soil moisture thresholds for vegetation function have been previously detected at the landscape scale (Bassiouni et al., 2020; Feldman et al., 2018).

3.4. Implications

Recent work showed that annual NEP is sensitive to interannual variations in rainfall totals and their projected changes (Gherardi & Sala, 2019; Maurer et al., 2020; Sala et al., 2015). However, reduced frequency and higher intensity rain events, apart from mean annual rainfall changes, are broadly expected under climate change (Knapp et al., 2008; Sala et al., 2015). Our findings show that vegetation across the US gradient of moisture availability shows significant carbon flux and water storage responses to pulses (Figures 2 and 3). Vegetation in drier environments is further sensitive to rain pulse characteristics, such as antecedent soil moisture and pulse magnitude (Figure 5). Therefore, changes in rain pulse characteristics under climate change can conceivably impact regional-to-global water, energy, and carbon balances.

It is ultimately unclear whether the projected less frequent, more intense rainfall will increase or decrease annual carbon sequestration. Some rainfall manipulation field experiments shifting rain intensity and frequency while holding total rainfall constant showed increases in primary production (Heisler-White et al., 2008; Knapp et al., 2002; Thomey et al., 2011). Others with a similar manipulation showed no change or decreases in primary production (Y. B. Hao et al., 2017; Harper et al., 2005; Liu et al., 2017). These differing experimental results may be due to competing physical processes. Larger rain events create deeper

infiltration (shifting soil water availability deeper, Sala et al., 2015) and induce longer plant productivity responses, but longer interevent drying periods reduce overall productivity and result in lagged responses after the next event (Liu et al., 2017; Plaut et al., 2013). We suspect that evaluating fundamental plant hydraulic and leaf gas exchange responses to pulses may provide a framework to evaluate these competing processes and potentially reconcile these experiments upon temporally upscaling to annual scales.

4. Summary and Conclusions

We use satellite-based landscape-scale plant water content and tower-based ecosystem-scale carbon flux measurements to evaluate vegetation responses to rain pulses across the continental United States. Our results are entirely observation driven, with observed pulse behavior not confounded by process-model assumptions. We find that plant water content and carbon fluxes show significant changes following moisture pulses across the US dry to humid climate gradient—not only in drylands where pulse field experiments have been primarily carried out. However, after aggregating sites into dryland and mesic environment groups, drylands show more frequent, longer plant water content and carbon flux responses following rain pulses. After further partitioning behavior based on pulse characteristics, only dryland vegetation tends to show discernable sensitivity to antecedent moisture and pulse magnitude. Specifically, large pulses and wet initial conditions result in the largest and longest dryland plant water content and carbon flux increase responses, evidence for pulsed growth responses. In contrast, small pulses and dry initial conditions show no carbon flux change and immediate plant water content loss along with soil moisture. These differences are in part due to soil moisture thresholds, below which plants are unable to upregulate, as found here primarily in drylands.

Ultimately, this study extends the assessment of vegetation pulse responses to a landscape scale across a dry to humid climatic gradient. It identifies similarities in plant responsiveness to pulse characteristics observed in independent carbon flux and plant water content metrics. Our results, therefore, show that novel satellite VOD observations hold meaningful vegetation information at daily to weekly time scales similarly to observed signatures in tower carbon flux measurements. Additionally, the study shows further evidence for soil moisture thresholds in both satellite and tower observations that a moisture pulse needs to exceed in order for primary production and water uptake responses to occur. These results have implications for how ecosystem plant behavior scales up to describe seasonal and annual primary production and vegetation sensitivity to rainfall characteristics.

Data Availability Statement

SMAP L1C brightness temperature used to retrieve soil moisture and vegetation optical depth are available from the National Snow and Ice Data Center (NSIDC) (https://nsidc.org/data/SPL1CTB_E). This work used eddy covariance data acquired and shared by the FLUXNET community.

References

Ainsworth, E. A., & Long, S. P. (2005). What have we learned from 15 years of free-air CO_2 enrichment (FACE)? A meta-analytic review of the responses of photosynthesis, canopy properties and plant production to rising CO_2. *New Phytologist*, *165*, 351–371. https://doi.org/10.1111/j.1469-8137.2004.01224.x

Akbar, R., Short Gianotti, D. J., McColl, K. A., Haghighi, E., Salvucci, G. D., & Entekhabi, D. (2018). Estimation of landscape soil water losses from satellite observations of soil moisture. *Journal of Hydrometeorology*, *19*, 871–889. https://doi.org/10.1175/JHM-D-17-0200.1

Angert, A. L., Huxman, T. E., Barron-Gafford, G. A., Gerst, K. L., & Venable, D. L. (2007). Linking growth strategies to long-term population dynamics in a guild of desert annuals. *Journal of Ecology*, *95*, 321–331. https://doi.org/10.1111/j.1365-2745.2006.01203.x

Baldocchi, D. D., Xu, L., & Kiang, N. (2004). How plant functional-type, weather, seasonal drought, and soil physical properties alter water and energy fluxes of an oak-grass savanna and an annual grassland. *Agricultural and Forest Meteorology*, *123*, 13–39. https://doi.org/10.1016/j.agrformet.2003.11.006

Bassiouni, M., Good, S. P., Still, C. J., & Higgins, C. W. (2020). Plant water uptake thresholds inferred from satellite soil moisture. *Geophysical Research Letters*, *47*, e2020GL087077. https://doi.org/10.1029/2020gl087077

Bernacchi, C. J., Kimball, B. A., Quarles, D. R., Long, S. P., & Ort, D. R. (2007). Decreases in stomatal conductance of soybean under open-air elevation of [CO_2] are closely coupled with decreases in ecosystem evapotranspiration. *Plant Physiology*, *143*, 134–144. https://doi.org/10.1104/pp.106.089557

Billesbach, D., Bradford, J., & Torn, M. (2012a). *FLUXNET2015 US-AR1 ARM USDA UNL OSU woodward switchgrass 1*, Dataset. 2009–2012. https://doi.org/10.18140/FLX/1440103

Billesbach, D., Bradford, J., & Torn, M. (2012b). *FLUXNET2015 US-AR2 ARM USDA UNL OSU woodward switchgrass 2*, Dataset. 2009–2012. https://doi.org/10.18140/FLX/1440104

Blackman, C. J., Brodribb, T. J., & Jordan, G. J. (2009). Leaf hydraulics and drought stress: Response, recovery and survivorship in four woody temperate plant species. *Plant, Cell and Environment*, *32*, 1584–1595. https://doi.org/10.1111/j.1365-3040.2009.02023.x

Bowling, D. (2007). *FLUXNET2015 US-cop corral pocket*. Dataset. 2001–2007. https://doi.org/10.18140/FLX/1440100

Brandt, M., Wigneron, J. P., Chave, J., Tagesson, T., Penuelas, J., Ciais, P., et al. (2018). Satellite passive microwaves reveal recent climate-induced carbon losses in African drylands. *Nature Ecology & Evolution*, *2*, 827–835. https://doi.org/10.1038/s41559-018-0530-6

Brodribb, T. J., & Cochard, H. (2009). Hydraulic failure defines the recovery and point of death in water-stressed conifers. *Plant Physiology*, *149*, 575–584. https://doi.org/10.1104/pp.108.129783

Burns, S. P., Blanken, P. D., Turnipseed, A. A., Hu, J., & Monson, R. K. (2015). The influence of warm-season precipitation on the diel cycle of the surface energy balance and carbon dioxide at a Colorado subalpine forest site. *Biogeosciences*, *12*, 7349–7377. https://doi.org/10.5194/bg-12-7349-2015

Carminati, A., Benard, P., Ahmed, M. A., & Zarebanadkouki, M. (2017). Liquid bridges at the root-soil interface. *Plant and Soil*, *417*, 1–15. https://doi.org/10.1007/s11104-017-3227-8

Carminati, A., Moradi, A. B., Vetterlein, D., Vontobel, P., Lehmann, E., Weller, U., et al. (2010). Dynamics of soil water content in the rhizosphere. *Plant and Soil*, *332*, 163–176. https://doi.org/10.1007/s11104-010-0283-8

Cavanaugh, M. L., Kurc, S. A., & Scott, R. L. (2011). Evapotranspiration partitioning in semiarid shrubland ecosystems: A two-site evaluation of soil moisture control on transpiration. *Ecohydrology*, *4*, 671–681. https://doi.org/10.1002/eco

Chan, S. K., Bindlish, R., O'Neill, P. E., Njoku, E., Jackson, T., Colliander, A., et al. (2016). Assessment of the SMAP passive soil moisture product. *IEEE Transactions on Geoscience and Remote Sensing*, *54*, 4994–5007. https://doi.org/10.1109/TGRS.2016.2561938

Chen, S., Lin, G., Huang, J., & Jenerette, D. (2009). Dependence of carbon sequestration on the differential responses of ecosystem photosynthesis and respiration to rain pulses in a semiarid steppe. *Global Change Biology*, *15*, 2450–2461. https://doi.org/10.1111/j.1365-2486.2009.01879.x

Chu, H., Chen, J., Gottgens, J. F., Desai, A. R., Ouyang, Z., & Qian, S. S. (2016). Response and biophysical regulation of carbon dioxide fluxes to climate variability and anomaly in contrasting ecosystems in northwestern Ohio, USA. *Agricultural and Forest Meteorology*, *220*, 50–68. https://doi.org/10.1016/j.agrformet.2016.01.008

Collins, S. L., Belnap, J., Grimm, N. B., Rudgers, J. A., Dahm, C. N., D'Odorico, P., et al. (2014). A multiscale, hierarchical model of pulse dynamics in arid-land ecosystems. *Annual Review of Ecology, Evolution and Systematics*, *45*, 397–419. https://doi.org/10.1146/annurev-ecolsys-120213-091650

Cook, B. D., Davis, K. J., Wang, W., Desai, A., Berger, B. W., Teclaw, R. M., et al. (2004). Carbon exchange and venting anomalies in an upland deciduous forest in northern Wisconsin, USA. *Agricultural and Forest Meteorology*, *126*, 271–295. https://doi.org/10.1016/j.agrformet.2004.06.008

Davis, K. J., Bakwin, P. S., Yi, C., Berger, B. W., Zhao, C., Teclaw, R. M., & Isebrands, J. G. (2003). The annual cycles of CO_2 and H_2O exchange over a northern mixed forest as observed from a very tall tower. *Global Change Biology*, *9*, 1278–1293. https://doi.org/10.1046/j.1365-2486.2003.00672.x

Desai, A. R., Bolstad, P. V., Cook, B. D., Davis, K. J., & Carey, E. V. (2005). Comparing net ecosystem exchange of carbon dioxide between an old-growth and mature forest in the upper Midwest, USA. *Agricultural and Forest Meteorology*, *128*, 33–55. https://doi.org/10.1016/j.agrformet.2004.09.005

Donovan, L., Linton, M., & Richards, J. (2001). Predawn plant water potential does not necessarily equilibrate with soil water potential under well-watered conditions. *Oecologia*, *129*, 328–335. https://doi.org/10.1007/s004420100738

Eagleson, P. S. (1978). Climate, soil, and vegetation 4. The expected value of annual evapotranspiration. *Water Resources Research*, *14*, 731–739.

Entekhabi, D., Njoku, E. G., O'Neill, P. E., Kellogg, K. H., Crow, W. T., Edelstein, W. N., et al. (2010). The soil moisture active passive (SMAP) mission. *Proceedings of the IEEE*, *98*, 704–716. https://doi.org/10.1109/JPROC.2010.2043918

Fares, S., Weber, R., Park, J. H., Gentner, D., Karlik, J., & Goldstein, A. H. (2012). Ozone deposition to an orange orchard: Partitioning between stomatal and non-stomatal sinks. *Environmental Pollution*, *169*, 258–266. https://doi.org/10.1016/j.envpol.2012.01.030

Feldman, A. F., Short Gianotti, D. J., Konings, A. G., McColl, K. A., Akbar, R., Salvucci, G. D., & Entekhabi, D. (2018). Moisture pulse-reserve in the soil–plant continuum observed across biomes. *Native Plants*, *4*, 1026–1033. https://doi.org/10.1038/s41477-018-0304-9

Feldman, A. F., Short Gianotti, D. J., Trigo, I. F., Salvucci, G. D., & Entekhabi, D. (2019). Satellite-based assessment of land surface energy partitioning–soil moisture relationships and effects of confounding variables. *Water Resources Research*, *55*, 10657–10677. https://doi.org/10.1029/2019WR025874

Fisher, J. B., Baldocchi, D. D., Misson, L., Dawson, T. E., & Goldstein, A. H. (2007). What the towers don't see at night: Nocturnal sap flow in trees and shrubs at two AmeriFlux sites in California. *Tree physiology*, *27*(4), 597–610. https://doi.org/10.1093/treephys/27.4.597

Frank, J. M., Massman, W. J., Ewers, B. E., Huckaby, L. S., & Negrón, J. F. (2014). Ecosystem CO_2/H_2O fluxes are explained by hydraulically limited gas exchange during tree mortality from spruce bark beetles. *Journal of Geophysical Research: Biogeosciences*, *119*, 1195–1215. https://doi.org/10.1002/2013JG002597

Fravolini, A., Hultine, K. R., Brugnoli, E., Gazal, R., English, N. B., & Williams, D. G. (2005). Precipitation pulse use by an invasive woody legume: The role of soil texture and pulse size. *Oecologia*, *144*, 618–627. https://doi.org/10.1007/s00442-005-0078-4

Gessler, A., Schaub, M., & McDowell, N. G. (2017). The role of nutrients in drought-induced tree mortality and recovery. *New Phytologist*, *214*, 513–520. https://doi.org/10.1111/nph.14340

Gherardi, L. A., & Sala, O. E. (2019). Effect of interannual precipitation variability on dryland productivity: A global synthesis. *Global Change Biology*, *25*, 269–276. https://doi.org/10.1111/gcb.14480

Goldstein, A. H., Hultman, N. E., Fracheboud, J. M., Bauer, M. R., Panek, J. A., Xu, M., et al. (2000). Effects of climate variability on the carbon dioxide, water, and sensible heat fluxes above a ponderosa pine plantation in the Sierra Nevada (CA). *Agricultural and Forest Meteorology*, *101*, 113–129. https://doi.org/10.1016/S0168-1923(99)00168-9

Gough, C. M., Hardiman, B. S., Nave, L. E., Bohrer, G., Kyle, D., Vogel, C. S., et al. (2013). Sustained carbon uptake and storage following moderate disturbance in a Great Lakes forest. *Ecological Applications*, *23*(5), 1202–1215.

Guo, Q., Li, S., Hu, Z., Zhao, W., Yu, G., Sun, X., et al. (2016). Responses of gross primary productivity to different sizes of precipitation events in a temperate grassland ecosystem in Inner Mongolia, China. *Journal of Arid Land*, *8*, 36–46. https://doi.org/10.1007/s40333-015-0136-7

Guo, J. S., & Ogle, K. (2019). Antecedent soil water content and vapor pressure deficit interactively control water potential in *Larrea tridentata*. *New Phytologist*, *221*, 218–232. https://doi.org/10.1111/nph.15374

Hao, Y., Wang, Y., Mei, X., Cui, X., Ecology, S. P., Issue, S., et al. (2010). The response of ecosystem CO_2 exchange to small precipitation pulses over a temperate steppe. *Plant Ecology*, *209*, 335–347.

Hao, Y. B., Zhou, C. T., Liu, W. J., Li, L. F., Kang, X. M., Jiang, L. L., et al. (2017). Aboveground net primary productivity and carbon balance remain stable under extreme precipitation events in a semiarid steppe ecosystem. *Agricultural and Forest Meteorology*, *240–241*, 1–9. https://doi.org/10.1016/j.agrformet.2017.03.006

Harper, C. W., Blair, J. M., Fay, P. A., Knapp, A. K., & Carlisle, J. D. (2005). Increased rainfall variability and reduced rainfall amount decreases soil CO_2 flux in a grassland ecosystem. *Global Change Biology*, *11*, 322–334. https://doi.org/10.1111/j.1365-2486.2005.00899.x

Heisler-White, J. L., Knapp, A. K., & Kelly, E. F. (2008). Increasing precipitation event size increases aboveground net primary productivity in a semi-arid grassland. *Oecologia*, *158*, 129–140. https://doi.org/10.1007/s00442-008-1116-9

Hollinger, D. Y., Ollingerw, S. V., Richardsonw, A. D., Meyersz, T. P., Dail, D. B., Martinw, M. E., et al. (2010). Albedo estimates for land surface models and support for a new paradigm based on foliage nitrogen concentration. *Global Change Biology*, *16*, 696–710. https://doi.org/10.1111/j.1365-2486.2009.02028.x

Huffman, G. (2015). . *GPM level 3 IMERG final run half hourly 0.1 × 0.1 degree precipitation, version 05*, Greenbelt, MD: Goddard Space Flight Center Distributed Active Archive Center (GSFC DAAC).

Huxman, T. E., Cable, J. M., Ignace, D. D., Eilts, J. A., English, N. B., Weltzin, J., & Williams, D. G. (2004). Response of net ecosystem gas exchange to a simulated precipitation pulse in a semi-arid grassland: The role of native versus non-native grasses and soil texture. *Oecologia*, *141*, 295–305. https://doi.org/10.1007/s00442-003-1389-y

Huxman, T. E., Snyder, K. A., Tissue, D., Leffler, A. J., Ogle, K., Pockman, W. T., et al. (2004). Precipitation pulses and carbon fluxes in semiarid and arid ecosystems. *Oecologia*, *141*, 254–268. https://doi.org/10.1007/s00442-004-1682-x

Ignace, D. D., Huxman, T. E., Weltzin, J. F., & Williams, D. G. (2007). Leaf gas exchange and water status responses of a native and non-native grass to precipitation across contrasting soil surfaces in the Sonoran Desert. *Oecologia*, *152*, 401–413. https://doi.org/10.1007/s00442-007-0670-x

Jackson, T. J., & Schmugge, T. J. (1991). Vegetation effects on the microwave emission of soils. *Remote Sensing of Environment*, *36*, 203–212. https://doi.org/10.1016/0034-4257(91)90057-D

Jarvis, P. G. (1976). The interpretation of the variations in leaf water potential and stomatal conductance found in canopies in the field. *Philosophical Transactions of the Royal Society B*, *273*, 593–610. https://doi.org/10.1098/rstb.1976.0035

Jarvis, P., Rey, A., Petsikos, C., Wingate, L., Rayment, M., Pereira, J., et al. (2007). Drying and wetting of Mediterranean soils stimulates decomposition and carbon dioxide emission: The "Birch effect". *Tree Physiology*, *27*, 929–940. https://doi.org/10.1093/treephys/27.7.929

Jasechko, S., Sharp, Z. D., Gibson, J. J., Birks, S. J., Yi, Y., & Fawcett, P. J. (2013). Terrestrial water fluxes dominated by transpiration. *Nature*, *496*, 347–350. https://doi.org/10.1038/nature11983

Jenerette, G. D., Scott, R. L., & Huxman, T. E. (2008). Whole ecosystem metabolic pulses following precipitation events. *Functional Ecology*, *22*, 924–930. https://doi.org/10.1111/j.1365-2435.2008.01450.x

Kerr, Y., Waldteufel, P., Wigneron, J.-P., Delwart, S., Cabot, F., Boutin, J., et al. (2010). The SMOS Mission : New tool for monitoring key elements of the global water cycle. *Proceedings of the IEEE*, *98*, 666–687.

Kim, S. (2013). *Ancillary data report: Landcover classification (JPL D-53057)*. Pasadena, CA: Jet Propulsion Laboratory California Institute of Technology.

Knapp, A. K., Beier, C., Briske, D. D., Classen, A. T., Luo, Y., Reichstein, M., et al. (2008). Consequences of more extreme precipitation regimes for terrestrial ecosystems. *BioScience*, *58*, 811–821. https://doi.org/10.1641/b580908

Knapp, A. K., Fay, P. A., Blair, J. M., Collins, S. L., Smith, M. D., Carlisle, J. D., et al. (2002). Rainfall variability, carbon cycling, and plant species diversity in a mesic grassland. *Science*, *298*(80), 2202–2205. https://doi.org/10.1126/science.1076347

Knox, S. H., Sturtevant, C., Matthes, J. H., Koteen, L., Verfaillie, J., & Baldocchi, D. (2015). Agricultural peatland restoration: Effects of land-use change on greenhouse gas (CO_2 and CH_4) fluxes in the Sacramento-San Joaquin Delta. *Global Change Biology*, *21*, 750–765. https://doi.org/10.1111/gcb.12745

Konings, A. G., Piles, M., Rotzer, K., McColl, K. A., Chan, S. K., & Entekhabi, D. (2016). Vegetation optical depth and scattering albedo retrieval using time series of dual-polarized L-band radiometer observations. *Remote Sensing of Environment*, *172*, 178–189. https://doi.org/10.1016/j.rse.2015.11.009

Konings, A. G., Rao, K., & Steele-Dunne, S. C. (2019). Macro to micro: Microwave remote sensing of plant water content for physiology and ecology. *New Phytologist*, *223*, 1166–1172. https://doi.org/10.1111/nph.15808

Koster, R. D., Schubert, S. D., & Suarez, M. J. (2009). Analyzing the concurrence of meteorological droughts and warm periods, with implications for the determination of evaporative regime. *Journal of Climate*, *22*, 3331–3341. https://doi.org/10.1175/2008JCLI2718.1

Kramer, P. J., & Boyer, J. S. (1995). *Water relations of plants and soils*, San Diego, CA: Academic Press.

Kurc, S. A., & Small, E. E. (2007). Soil moisture variations and ecosystem-scale fluxes of water and carbon in semiarid grassland and shrubland. *Water Resources Research*, *43*, W06416. https://doi.org/10.1029/2006WR005011

Law, B. E., Falge, E., Gu, L., Baldocchi, D. D., Bakwin, P., Berbigier, P., et al. (2002). Environmental controls over carbon dioxide and water vapor exchange of terrestrial vegetation. *Agricultural and Forest Meteorology*, *113*, 97–120. https://doi.org/10.1016/S0168-1923(02)00104-1

Law, B. E., Turner, D., Campbell, J., Sun, O. J., Van Tuyl, S., Ritts, W. D., & Cohen, W. B. (2004). Disturbance and climate effects on carbon stocks and fluxes across Western Oregon USA. *Global Change Biology*, *10*, 1429–1444. https://doi.org/10.1111/j.1365-2486.2004.00822.x

Li, J. H., Dijkstra, P., Hinkle, C. R., Wheeler, R. M., & Drake, B. G. (1999). Photosynthetic acclimation to elevated atmospheric CO_2 concentration in the Florida scrub-oak species *Quercus geminata* and *Quercus myrtifolia* growing in their native environment. *Tree Physiology*, *19*, 229–234. https://doi.org/10.1093/treephys/19.4-5.229

Liu, W. J., Li, L. F., Biederman, J. A., Hao, Y. B., Zhang, H., Kang, X. M., et al. (2017). Repackaging precipitation into fewer, larger storms reduces ecosystem exchanges of CO_2 and H_2O in a semiarid steppe. *Agricultural and Forest Meteorology*, *247*, 356–364. https://doi.org/10.1016/j.agrformet.2017.08.029

Lo Gullo, M. A., Nardini, A., Salleo, S., & Tyree, M. T. (1998). Changes in root hydraulic conductance (K(R)) of Olea oleaster seedlings following drought stress and irrigation. *New Phytologist*, *140*, 25–31. https://doi.org/10.1046/j.1469-8137.1998.00258.x

Loik, M. E. (2007). Sensitivity of water relations and photosynthesis to summer precipitation pulses for *Artemisia tridentata* and *Purshia tridentata*. *Plant Ecology*, *191*, 95–108. https://doi.org/10.1007/s11258-006-9217-1

Madani, N., Kimball, J. S., Jones, L. A., Parazoo, N. C., & Guan, K. (2017). Global analysis of bioclimatic controls on ecosystem productivity using satellite observations of solar-induced chlorophyll fluorescence. *Remote Sensing*, *9*, 530. https://doi.org/10.3390/rs9060530

Martorell, S., Diaz-Espejo, A., Medrano, H., Ball, M. C., & Choat, B. (2014). Rapid hydraulic recovery in *Eucalyptus pauciflora* after drought: Linkages between stem hydraulics and leaf gas exchange. *Plant, Cell and Environment*, *37*, 617–626. https://doi.org/10.1111/pce.12182

Maurer, G. E., Hallmark, A. J., Brown, R. F., Sala, O. E., & Collins, S. L. (2020). Sensitivity of primary production to precipitation across the United States. *Ecology Letters*, *23*, 527–536. https://doi.org/10.1111/ele.13455

McColl, K. A., Wang, W., Peng, B., Akbar, R., Short Gianotti, D. J., Lu, H., et al. (2017). Global characterization of surface soil moisture drydowns. *Geophysical Research Letters*, *44*, 3682–3690. https://doi.org/10.1002/2017GL072819

Meyers, T. P. (2001). A comparison of summertime water and CO_2 fluxes over rangeland for well watered and drought conditions. *Agricultural and Forest Meteorology*, *106*, 205–214. https://doi.org/10.1016/S0168-1923(00)00213-6

Miao, A. S. L., & Bazzaz, F. A. (1990). Responses to nutrient pulses of two colonizers requiring different disturbance frequencies. *Ecology*, *71*, 2166–2178.

Momen, M., Wood, J. D., Novick, K. A., Pangle, R., Pockman, W. T., McDowell, N. G., & Konings, A. G. (2017). Interacting effects of leaf water potential and biomass on vegetation optical depth. *Journal of Geophysical Research: Biogeosciences*, *122*, 3031–3046. https://doi.org/10.1002/2017JG004145

Myneni, R., Knyazikhin, Y., & Park, T. (2015). MOD15A2H MODIS leaf area index/FPAR 8-day L4 global 500m SIN grid V006. NASA EOSDIS Land Processes DAAC.

Nemani, R. R., Keeling, C. D., Hashimoto, H., Jolly, W. M., Piper, S. C., Tucker, C. J., et al. (2003). Climate-driven increases in global terrestrial net primary production from 1982 to 1999. *Science*, *300*, 1560–1563. https://doi.org/10.1126/science.1082750

North, G. B., & Nobel, P. S. (1991). Changes in hydraulic conductivity and anatomy caused by drying and rewetting roots of *Agave deserti* (Agavaceae). *American Journal of Botany*, *78*, 906. https://doi.org/10.2307/2445169

North, G. B., & Nobel, P. S. (1997). Root-soil contact for the desert succulent *Agave deserti* in wet and drying soil. *New Phytologist*, *135*, 21–29. https://doi.org/10.1046/j.1469-8137.1997.00620.x

Novick, K. A., Ficklin, D. L., Stoy, P. C., Williams, C. A., Bohrer, G., Oishi, A. C., et al. (2016). The increasing importance of atmospheric demand for ecosystem water and carbon fluxes. *Nature Climate Change*, *6*, 1023–1027. https://doi.org/10.1038/nclimate3114

Novoplansky, A., & Goldberg, D. E. (2001). Effects of water pulsing on individual performance and competitive hierarchies in plants. *Journal of Vegetable Science*, *12*, 199–208. https://doi.org/10.2307/3236604

Noy-Meir, I. (1973). Desert ecosystems: Environment and producers. *Annual Review of Ecology and Systematics*, *4*, 25–52.

Ogle, K., & Reynolds, J. F. (2004). Plant responses to precipitation in desert ecosystems: Integrating functional types, pulses, thresholds, and delays. *Oecologia*, *141*, 282–294. https://doi.org/10.1007/s00442-004-1507-5

Oikawa, P. Y., Sturtevant, C., Knox, S. H., Verfaillie, J., Huang, Y. W., & Baldocchi, D. D. (2017). Revisiting the partitioning of net ecosystem exchange of CO_2 into photosynthesis and respiration with simultaneous flux measurements of $^{13}CO_2$ and CO_2, soil respiration and a biophysical model, CANVEG. *Agricultural and Forest Meteorology*, *234–235*, 149–163. https://doi.org/10.1016/j.agrformet.2016.12.016

Pastorello, G. (2020). The FLUXNET2015 dataset and the ONEFlux processing pipeline for eddy covariance data. *Scientific Data*, *7*, 225.

Phillips, N. G., Oren, R., Licata, J., & Linder, S. (2004). Time series diagnosis of tree hydraulic characteristics. *Tree Physiology*, *24*, 879–890. https://doi.org/10.1093/treephys/24.8.879

Plaut, J. A., Wadsworth, W. D., Pangle, R., Yepez, E. A., Mcdowell, N. G., & Pockman, W. T. (2013). Reduced transpiration response to precipitation pulses precedes mortality in a piñon-juniper woodland subject to prolonged drought. *New Phytologist*, *200*, 375–387. https://doi.org/10.1111/nph.12392

Pockman, W. T., & Small, E. E. (2010). The influence of spatial patterns of soil moisture on the grass and shrub responses to a summer rainstorm in a Chihuahuan desert ecotone. *Ecosystems*, *13*, 511–525. https://doi.org/10.1007/s10021-010-9337-2

Post, A. K., & Knapp, A. K. (2019). Plant growth and aboveground production respond differently to late-season deluges in a semi-arid grassland. *Oecologia*, *191*, 673–683. https://doi.org/10.1007/s00442-019-04515-9

Potts, D. L., Barron-Gafford, G. A., & Jenerette, G. D. (2014). Metabolic acceleration quantifies biological systems' ability to up-regulate metabolism in response to episodic resource availability. *Journal of Arid Environments*, *104*, 9–16. https://doi.org/10.1016/j.jaridenv.2014.01.018

Potts, D. L., Huxman, T. E., Cable, J. M., English, N. B., Ignace, D. D., Eilts, J. A., et al. (2006). Antecedent moisture and seasonal precipitation influence the response of canopy-scale carbon and water exchange to rainfall pulses in a semi-arid grassland. *New Phytologist*, *170*, 849–860. https://doi.org/10.1111/j.1469-8137.2006.01732.x

Raz-Yaseef, N., Billesbach, D. P., Fischer, M. L., Biraud, S. C., Gunter, S. A., Bradford, J. A., & Torn, M. S. (2015). Vulnerability of crops and native grasses to summer drying in the U.S. Southern Great Plains. *Agriculture, Ecosystems & Environment*, *213*, 209–218. https://doi.org/10.1016/j.agee.2015.07.021

Reed, D. E., Ewers, B. E., Pendall, E., Naithani, K. J., Kwon, H., & Kelly, R. D. (2018). Biophysical factors and canopy coupling control ecosystem water and carbon fluxes of semiarid sagebrush ecosystems. *Rangeland Ecology & Management*, *71*, 309–317. https://doi.org/10.1016/j.rama.2018.01.003

Reynolds, J. F., Kemp, P. R., Ogle, K., & Fernández, R. J. (2004). Modifying the "pulse-reserve" paradigm for deserts of North America: Precipitation pulses, soil water, and plant responses. *Oecologia*, *141*, 194–210. https://doi.org/10.1007/s00442-004-1524-4

Richardson, A. D., Hollinger, D. Y., Burba, G. G., Davis, K. J., Flanagan, L. B., Katul, G. G., et al. (2006). A multi-site analysis of random error in tower-based measurements of carbon and energy fluxes. *Agricultural and Forest Meteorology*, *136*, 1–18. https://doi.org/10.1016/j.agrformet.2006.01.007

Roby, M. C., Scott, R. L., & Moore, D. J. P. (2020). High vapor pressure deficit decreases the productivity and water-use efficiency of rain-induced pulses in semiarid ecosystems. *Journal of Geophysical Research: Biogeosciences*, *125*, e2020JG005665. https://doi.org/10.1029/2020JG005665

Roman, D. T., Novick, K. A., Brzostek, E. R., Dragoni, D., Rahman, F., & Phillips, R. P. (2015). The role of isohydric and anisohydric species in determining ecosystem-scale response to severe drought. *Oecologia*, *179*, 641–654. https://doi.org/10.1007/s00442-015-3380-9

Ruehr, N. K., Martin, J. G., & Law, B. E. (2012). Effects of water availability on carbon and water exchange in a young ponderosa pine forest: Above- and belowground responses. *Agricultural and Forest Meteorology*, *164*, 136–148. https://doi.org/10.1016/j.agrformet.2012.05.015

Sala, O. E., Gherardi, L. A., & Peters, D. P. C. (2015). Enhanced precipitation variability effects on water losses and ecosystem functioning: Differential response of arid and mesic regions. *Climatic Change*, *131*, 213–227. https://doi.org/10.1007/s10584-015-1389-z

Sala, O. E., & Lauenroth, W. K. (1982). Small rainfall events: An ecological role in semiarid regions. *Oecologia*, *53*, 301–304.

Schwinning, S., & Sala, O. E. (2004). Hierarchy of responses to resource pulses in arid and semi-arid ecosystems. *Oecologia*, *141*, 211–220. https://doi.org/10.1007/s00442-004-1520-8

Schwinning, S., Sala, O. E., Loik, M. E., & Ehleringer, J. R. (2004). Thresholds, memory, and seasonality: Understanding pulse dynamics in arid/semi-arid ecosystems. *Oecologia*, *141*, 191–193. https://doi.org/10.1007/s00442-004-1683-3

Schwinning, S., Starr, B. I., & Ehleringer, J. R. (2003). Dominant cold desert plants do not partition warm season precipitation by event size. *Oecologia*, *136*, 252–260. https://doi.org/10.1007/s00442-003-1255-y

Scott, R. L., Biederman, J. A., Hamerlynck, E. P., & Barron-Gafford, G. A. (2015). The carbon balance pivot point of southwestern U.S. semiarid ecosystems: Insights from the 21st century drought. *Journal of Geophysical Research: Biogeosciences*, *120*, 2612–2624. https://doi.org/10.1002/2015JG003181

Scott, R. L., Huxman, T. E., Cable, W. L., & Emmerich, W. E. (2006). Partitioning of evapotranspiration and its relation to carbon dioxide exchange in a Chihuahuan Desert shrubland. *Hydrological Processes*, *20*, 3227–3243. https://doi.org/10.1002/hyp.6329

Sher, A. A., Goldberg, D. E., & Novoplansky, A. (2004). The effect of mean and variance in resource supply on survival of annuals from Mediterranean and desert environments. *Oecologia*, *141*, 353–362. https://doi.org/10.1007/s00442-003-1435-9

Short Gianotti, D. J., Rigden, A. J., Salvucci, G. D., & Entekhabi, D. (2019). Satellite and station observations demonstrate water availability's effect on continental-scale evaporative and photosynthetic land surface dynamics. *Water Resources Research*, *55*, 540–554. https://doi.org/10.1029/2018WR023726

Akbar, R., McColl, K. A., Cuenca, R., & Entekhabi, D. (2019). Landscape water storage and subsurface correlation from satellite surface soil moisture and precipitation observations. *Water Resources Research*, *55*, 9111–9132. https://doi.org/10.1029/2019wr025332

Smith, W. K., Dannenberg, M. P., Yan, D., Herrmann, S., Barnes, M. L., Barron-Gafford, G. A., et al. (2019). Remote sensing of dryland ecosystem structure and function: Progress, challenges, and opportunities. *Remote Sensing of Environment*, *233*, 111401. https://doi.org/10.1016/j.rse.2019.111401

Tang, Y., Jiang, J., Chen, C., Chen, Y., & Wu, X. (2018). Rainfall pulse response of carbon fluxes in a temperate grass ecosystem in the semiarid Loess Plateau. *Ecology and Evolution*, *8*, 11179–11189. https://doi.org/10.1002/ece3.4587

Thomey, M. L., Collins, S. L., Vargas, R., Johnson, J. E., Brown, R. F., Natvig, D. O., & Friggens, M. T. (2011). Effect of precipitation variability on net primary production and soil respiration in a Chihuahuan Desert grassland Effect of precipitation variability on net primary production and soil respiration in a Chihuahuan Desert grassland. *Global Change Biology*, *17*, 1505–1515. https://doi.org/10.1111/j.1365-2486.2010.02363.x

Tian, F., Wigneron, J.-P., Ciais, P., Chave, J., Ogée, J., Peñuelas, J., et al. (2018). Coupling of ecosystem-scale plant water storage and leaf phenology observed by satellite. *Nature Ecology & Evolution*, *2*, 1428–1435. https://doi.org/10.1038/s41559-018-0630-3

Trifilò, P., Raimondo, F., Nardini, A., Lo Gullo, M. A., & Salleo, S. (2004). Drought resistance of *Ailanthus altissima*: Root hydraulics and water relations. *Tree Physiology*, *24*, 107–114. https://doi.org/10.1093/treephys/24.1.107

Vickers, D., Thomas, C., & Law, B. E. (2009). Random and systematic CO$_2$ flux sampling errors for tower measurements over forests in the convective boundary layer. *Agricultural and Forest Meteorology*, *149*, 73–83. https://doi.org/10.1016/j.agrformet.2008.07.005

Weltzin, J. F., Loik, M. E., Schwinning, S., Williams, D. G., Fay, P. A., Haddad, B. M., et al. (2003). Assessing the response of terrestrial ecosystems to potential changes in precipitation. *BioScience*, *53*, 941. https://doi.org/10.1641/0006-3568(2003)053[0941:ATROTE]2.0.CO;2

Weltzin, J. F., & Tissue, D. T. (2003). Resource pulses in arid environments—patterns of rain, patterns of life. *New Phytologist*, *157*, 171–173. https://doi.org/10.1046/j.1469-8137.2003.00672.x

West, A. G., Hultine, K. R., Jackson, T. L., & Ehleringer, J. R. (2007). Differential summer water use by *Pinus edulis* and *Juniperus osteosperma* reflects contrasting hydraulic characteristics. *Tree Physiology*, *27*, 1711–1720. https://doi.org/10.1093/treephys/27.12.1711

Williams, C. A., Hanan, N., Scholes, R. J., & Kutsch, W. (2009). Complexity in water and carbon dioxide fluxes following rain pulses in an African savanna. *Oecologia*, *161*, 469–480. https://doi.org/10.1007/s00442-009-1405-y

Xu, L., Baldocchi, D. D., & Tang, J. (2004). How soil moisture, rain pulses, and growth alter the response of ecosystem respiration to temperature. *Global Biogeochemical Cycles*, *18*, GB4002. https://doi.org/10.1029/2004GB002281

Yang, L. H., Bastow, J. L., Spence, K. O., & Wright, A. N. (2008). What can we learn from resource pulses? *Ecology*, *89*, 621–634.

Zhang, Y., Zhou, S., Gentine, P., & Xiao, X. (2019). Can vegetation optical depth reflect changes in leaf water potential during soil moisture dry-down events? *Remote Sensing of Environment*, *234*, 111451.